TECHNICAL REPORT STANDARD TITLE PAGE

1. Report No.	2. Government Accession No.	3. Recipient's Catalog No.

4. Title and Subtitle	5. Report Date
"Strength and Serviceability of Inverted T-Beam Bent Caps Subject to Combined Flexure, Shear, and Torsion"	August 1974
	6. Performing Organization Code
7. Author(s)	8. Performing Organization Report No.
Richard W. Furlong and Sher Ali Mirza	Research Report 153-1F
9. Performing Organization Name and Address	10. Work Unit No.
Center for Highway Research The University of Texas at Austin Austin, Texas 78712	11. Contract or Grant No. Research Study 3-5-71-153
	13. Type of Report and Period Covered
12. Sponsoring Agency Name and Address Texas Highway Department Planning & Research Division P. O. Box 5051 Austin, Texas 78763	Final September 1970 - August 1973
	14. Sponsoring Agency Code

15. Supplementary Notes

Work done in cooperation with the Federal Highway Administration, Department of Transportation. Research Study Title: Strength and Serviceability of Inverted T-Beam Bent Caps Subject to Combined Flexure, Shear, and Torsion

16. Abstract

Concrete inverted T-beams that support precast stringers on the flanges of the inverted T were studied in 27 load tests on seven specimens. Loading included combinations of flexural shear and torsional shear on prestressed and on nonprestressed specimens. Results provide advice for reinforcement details and design procedures applicable to the flanges as well as the shear and flexural strength of such beams.

17. Key Words	18. Distribution Statement
strength, serviceability, T-beam, concrete, flange, bent cap, flexural shear, torsional shear, prestressed, nonprestressed	

19. Security Classif. (of this report)	20. Security Classif. (of this page)	21. No. of Pages	22. Price
Unclassified	Unclassified	89	

Form DOT F 1700.7 (8-69)

STRENGTH AND SERVICEABILITY OF INVERTED T-BEAM BENT CAPS SUBJECT TO COMBINED FLEXURE, SHEAR, AND TORSION

By

Richard W. Furlong

and

Sher Ali Mirza

Research Report No. 153-1F

Research Project Number 3-5-71-153
Strength and Serviceability of Inverted T-Beam Bent Caps
Subject to Combined Flexure, Shear, and Torsion

Conducted for

The Texas Highway Department

In Cooperation with the
U. S. Department of Transportation
Federal Highway Administration

by

CENTER FOR HIGHWAY RESEARCH
THE UNIVERSITY OF TEXAS AT AUSTIN

August 1974

The contents of this report reflect the views of the authors, who are responsible for the facts and the accuracy of the data presented herein. The contents do not necessarily reflect the official views or policies of the Federal Highway Administration. This report does not constitute a standard, specification, or regulation.

P R E F A C E

This Research Report 153-1F is the final and only report of Research Project 3-5-71-153, Federal No. HPR-1(12), entitled "Strength and Serviceability of Inverted T-Beam Bent Caps Subject to Combined Flexure, Shear, and Torsion." The project was a sequel to an earlier study into problems associated with splices and anchorage of reinforcing bars (Project No. 3-5-68-113). Recommendations that were made from the earlier study, Research Report No. 113-4, "Shear and Anchorage Study of Reinforcement in Inverted T-Beam Bent Cap Girders," were incorporated into specimens used for this project.

Support has been provided by the Texas Highway Department and the Federal Highway Administration, United States Department of Transportation. The encouragement and assistance of their contact representatives, Leo K. Willis and D. E. Harley, are acknowledged with thanks.

R. W. Furlong
S. A. Mirza

A B S T R A C T

Concrete inverted T-beams that support precast stringers on the flanges of the inverted T were studied in 27 load tests on seven specimens. Loading included combinations of flexural shear and torsional shear on prestressed and on nonprestressed specimens. Results provide advice for reinforcement details and design procedures applicable to the flanges as well as the shear and flexural strength of such beams.

S U M M A R Y

Bent cap girders in the shape of an inverted T have been used with considerable success, particularly in structures at grade separations. As traffic approaches such bent caps, stringer reactions on one flange cause torsion or twisting toward the approaching load. After traffic passes the bent cap, it causes twisting in the opposite direction. At the present time (1974), the only North American standards for design of concrete subject to torsion are presented in the building Code of the American Concrete Institute and in the National Building Code of Canada. Standards are very similar in the two documents, but neither document includes recommendations for prestressed concrete members subject to torsion.

Observations from 27 load tests on seven specimens, four of which were prestressed, indicated that the present ACI and NBC procedures for assigning strength in flexural shear and torsion underestimated torsion strength by 50 percent. The tests also showed that prestressed concrete members exhibited under service loads less cracking and lower stresses in transverse reinforcement than did nonprestressed members with identical proportions.

Recommended design procedures and equations for assessing strength were proposed. The recommendations can be applied for the design of transverse reinforcement in prestressed or nonprestressed beams. Supplementary advice for the design of stirrups and for assessing flange depth requirements as each is limited by shear were made also.

RESEARCH IMPLEMENTATION

The results of this project include:

(1) Suggestions for recommended practice in the design of reinforcement to support torsion combined with flexural shear on prestressed concrete members.

(2) Equations for determining stirrup spacing requirements in the web of inverted T-beams.

(3) An equation and a graphical design aid for determining minimum thickness of flanges of inverted T-beams.

(4) A discussion and extension of recommendations in Ref. 1 for the design of transverse reinforcement in inverted T-beam flanges.

The recommendations for design are expressed in terms of Strength Design rather than Allowable Stress Design in order to promote easier correlation with background data published by the American Concrete Institute since 1965. It is felt that the findings of this research are sufficient to recommend the adoption of proposed design procedures applicable to inverted T-beams.

Task groups who are developing design standards for AASHTO and for ACI should be informed of test results and proposed design procedures from this study. It is possible that some of the existing design requirements for the use of steel can be made more efficient if results from other investigations indicate similar strength underestimates that are derived from existing required procedures. Some economy in design time may be made possible through the use of recommended procedures.

C O N T E N T S

L I S T O F T A B L E S

L I S T O F F I G U R E S

CHAPTER 1

INTRODUCTION

Inverted T-beams represent a natural and popular structural form for use as a girder to support precast beams. The flange of the inverted T serves as a shallow shelf to support beams while the stem of the inverted T, rising to the height of supported beams, provides the needed depth to sustain flexure and shear forces. Figure 1 illustrates how it presents a more attractive appearance at bridge supports by minimizing the visual interruption to longitudinal lines and shadows created by deck support members. Also, by keeping to a minimum the visible size of transverse supporting elements, the amount of light and headroom beneath the bridge deck are enhanced.

The structural behavior of the inverted T shape differs from that of the more traditional top-loaded "standard" T in the following ways:

(a) Loads that are introduced from beams into the bottom rather than into the sides or the top of the web must be supported by stirrups acting as hangers to transmit vertical forces into the body of the web.

(b) Flange reinforcement perpendicular to the web is necessary to deliver the flange forces to the hangers.

(c) The application of flange forces necessarily occurs at a greater distance from the centerline of the web, thereby creating greater torsional or twisting forces on the web.

Conclusions from Project 3-5-68-113 (Ref. 1) indicated that there was no superposition necessary for vertical flexural shear forces and vertical hanger forces. The possible aggravation of tensile forces and consequent cracking due to torsion in addition to hanger and flexural stresses was not investigated.

As traffic moves across an inverted T-beam bent cap, the stringers on one side of the web will create a web twist opposite to that which

Fig. 1. Some inverted T-beam bent cap girders in place.

occurs when the stringers on the opposite side of the web are loaded by the traffic. Of course the maximum, total vertical load on a bent cap should occur when stringers on both sides of the web simultaneously are supporting traffic. In the presence of significant torsion, flange forces on one side of the web must be significantly larger than forces on the opposite side of the web, and the passage of traffic tends to make such twisting an alternating phenomenon. The response of inverted T-beams to combined flexure and torsion requires observation for both service load and ultimate load conditions.

Load paths for tensile forces through cracked portions of reinforced concrete members can be assigned to reinforcement in order to define analytic models for design. Conventional reinforced concrete members tend to crack at relatively low levels of principal tension stress, and the existence of tensile strength in concrete can be neglected when analytic models are identified. The precompression of a concrete cross section can reduce and even eliminate tension stress. Consequently, the response of prestressed concrete members may be significantly different from that of conventionally reinforced concrete members subjected to the same conditions of combined torsional and flexural loading. Observations from tests on both conventionally reinforced and prestressed concrete members should be compared for purposes of improving design criteria.

This study was initiated to provide data useful for designing both conventional and prestressed inverted T-beam bent cap members. Special attention was given to:

(a) Web reinforcement, both the amount and the location of stirrups.

(b) Service load cracking in response to equal and opposite "live load" torsions.

(c) The strength and stiffness of web and flange as the amount of combined flexure, shear, and torsion was increased until a maximum capacity was reached.

Design Criteria for Inverted T-Beams

Applicable Design Specifications--1974. The principal document for guidance in the design of highway bridge structures in the United States is Ref. 2, Standard Specifications for Highway Bridges, American Association of State Highway Officials, Washington, D.C., 1973. The AASHO Specifications contain general design criteria for proportioning reinforced concrete members and criteria also for prestressed concrete members. The criteria are general in nature, referring specifically to flexural strength requirements and shear strength requirements for beams. The 1973 edition does not contain recommendations for the design of beams to resist torsion, nor does it contain recommendations specifically directed toward problems of deep beam behavior and very short bar development length associated with bracket design.

Both the subject of torsion and design recommendations for deep beams and brackets are incorporated in the 1971 edition of the Building Code of the American Concrete Institute.[3] The 1971 Building Code specifies load factor design criteria for all reinforced concrete members. The principal emphasis of the ACI Building Code is directed toward concrete components of buildings, not bridges. Special consideration of problems associated with exposure to weather and repetitive dynamic loading are not a part of the Building Code. Even so, the Building Code can be cited for the design of reinforced concrete bridge components subjected to torsion as well as components that contain brackets. The Building Code does not contain guidance for evaluating the torsional strength of prestressed concrete members. Since all regulations of the Building Code are in terms of load factor design strength, it can be used only in terms of ultimate strength design even for bridge members.

The AASHO Specifications contain separate sections that may be used for design. One section, called Allowable Stresses (Sec. 1.5.1), specifies upper limits for stresses estimated to occur under normal service load conditions. Another section of the AASHO Specifications, called Load Factor Design (Sec. 1.5.14), sets forth minimum requirements of ultimate strength necessary to resist factored loads. Reinforced

concrete bridge members can be proportioned on the basis of either the Allowable Stresses section or the Load Factor Design section. Members need not be checked to satisfy both. On the contrary, however, prestressed concrete members must be checked for service load stresses and, in addition, the ultimate strength of prestressed concrete members must be adequate to sustain factored loads on the structure. Section 6 of the 1973 AASHO Specifications applies to prestressed concrete beams. Section 6 requires that both allowable stress design and load factor design must be considered for prestressed concrete members. The requirements of Section 6 do not mention the existence of torsion.

Since the ultimate strength or load factor design procedure is a required part of prestressed concrete specifications for highway bridges, and for reinforced concrete members designed in accordance with the ACI Building Code, all test data accumulated in this project are correlated with design criteria in terms of load factor design. The most appropriate load factors appear to be those required in the 1973 edition of AASHO Specifications. The evaluation of capacity to resist torsional forces on reinforced concrete members and the capacity of inverted T-beam flanges acting as brackets can be based on regulations of the ACI Building Code. The evaluation of torsional strength of prestressed concrete beams cannot be based on either the ACI Building Code or the AASHO Specifications. Recommendations for evaluating the torsional strength of prestressed concrete beams, therefore, constitute a major goal of the research reported here. The Load Factor Design method in the 1973 AASHO Specifications and the 1971 ACI Building Code imply virtually the same criteria for the evaluation of flexural capacity and shear capacity in both reinforced concrete and prestressed concrete members. The magnitude of load factors required by AASHO Specifications differs from magnitudes required by the 1971 ACI Building Code. All of the design data for this report will be based on AASHO load factors for dead load and for loads from moving traffic. Reference will be made to AASHO strength criteria wherever possible, and ACI strength criteria will be cited in those instances for which no similar AASHO criteria exist.

Recommended Practice. Several aspects of the behavior of inverted T-beam bent cap girders cannot be classified to fit existing specifications for the design of reinforced concrete members. Three aspects of design already mentioned for special attention, i.e., (a) the amount and location of web stirrups, (b) service load cracking created by torsion, and (c) ultimate strength and stiffness under combined flexural and torsional loading on prestressed concrete, are aspects of structural behavior for which no specification exists.

Design advice for detailing reinforcement in the flanges of inverted T-beams most effectively to transmit to the web concentrated loads applied to the flange is available only from recent research.[1,4] The basic problem encountered for the proportioning of transverse reinforcement in flanges involves the assignment of an effective length or an effective region over which the reinforcement can be expected to help support a concentrated force applied to the flange. Criteria from Ref. 1 were used for specimens in the study reported here.

CHAPTER 2

PHYSICAL TESTS

The behavior of inverted T-beam elements subjected to combined flexure and torsional loading was observed from 27 tests to failure performed on three reinforced concrete and four prestressed concrete specimens. The specimens represented approximately one-third scale models of inverted T-beam bent cap girders similar to those used by the Texas Highway Department. The prototype bent cap girders had been proportioned to support dead load stringer reactions near 80 kips and live load and impact reactions of 120 kips at each stringer. For one-third scale models, the load similitude factor becomes one-ninth, such that nominal dead load stringer reactions on test specimens could be taken as 10 kips and live load stringer reactions could be taken as 15 kips.

Three basic test arrangements were employed in order to observe the response to: (a) loads that created positive moment combined with torsion and shear, (b) loads that caused negative moment combined with shear and torsion, and (c) loads that created pure torque. Some portions of prestressed concrete members were subjected to a torsional loading applied midway between torsionally clamped support regions. The principal variables employed in the experimental study were the reinforcement details associated with web shear and torsional strength. Some minor variations in the type of transverse reinforcement used for flanges were also employed. All of the laboratory specimens for this study had a cross section consisting of an 8 in. wide web, 21 in. deep, plus a flange that was 22 in. wide. Each side of the flange, therefore, extended 7 in. out from the face of the web. The flange of the first specimen tested was 6 in. thick, and a 7 in. thick flange was employed for all other specimens. A nominal 5/8 in. concrete cover at reinforcement corresponded with 3 x 5/8 = approximately 2 in. of cover for the prototype girders.

Failure regions for the laboratory specimens involved approximately one depth of the beam, or something near 2 ft. in the length of the member. Test loadings representative of stringer forces on the prototype girders required test specimens approximately 12 ft. long. At least twelve different configurations of loading and reinforcement were desired in the test program. Instead of fabricating twelve specimens, each to be loaded one time to failure, considerable savings were envisioned from the use of fewer specimens, each subjected to several different tests until failure in local regions. Seven specimens, each 24 ft. long, were fabricated and 27 individual tests to failure were conducted altogether.

Details of Test Specimens

Each specimen was identified with a label consisting of a T, representing the shape of the cross section; a second letter C or P, identifying the major type of longitudinal reinforcement (C = deformed bars only, P = prestressing cables plus deformed bars); a third symbol indicated the casting sequence of the specimen; and the last symbol indicated the sequence of individual tests performed on the specimen. Thus, TP32 designates the second test on the specimen cast third and reinforced longitudinally with prestressing cables and deformed bars.

The specific reinforcement details for the specimens are given with the sketches contained in Figs. 2 through 8. Along with the details of each specimen are shown sketches that indicate the placement of load for the tests that were performed on each specimen.

Specimen TC1, shown in Fig. 2, contained vertical stirrups at 6 in. centers through the central 10 ft. length of the specimen; #3 stirrups were placed at 4 in. centers in the end region. Longitudinal reinforcement consisted of ten #6 bars in the top of the stem and eleven #6 bars across the flange at the bottom of the specimen. Transverse reinforcement in the web was constant throughout the specimen, and it consisted of #3 bars at 3 in. centers in the top of the flange and #2 plain bars (not deformed steel) at midheight. A U-shaped #2 tie extended across the bottom of the flange and up each side of the flange. The

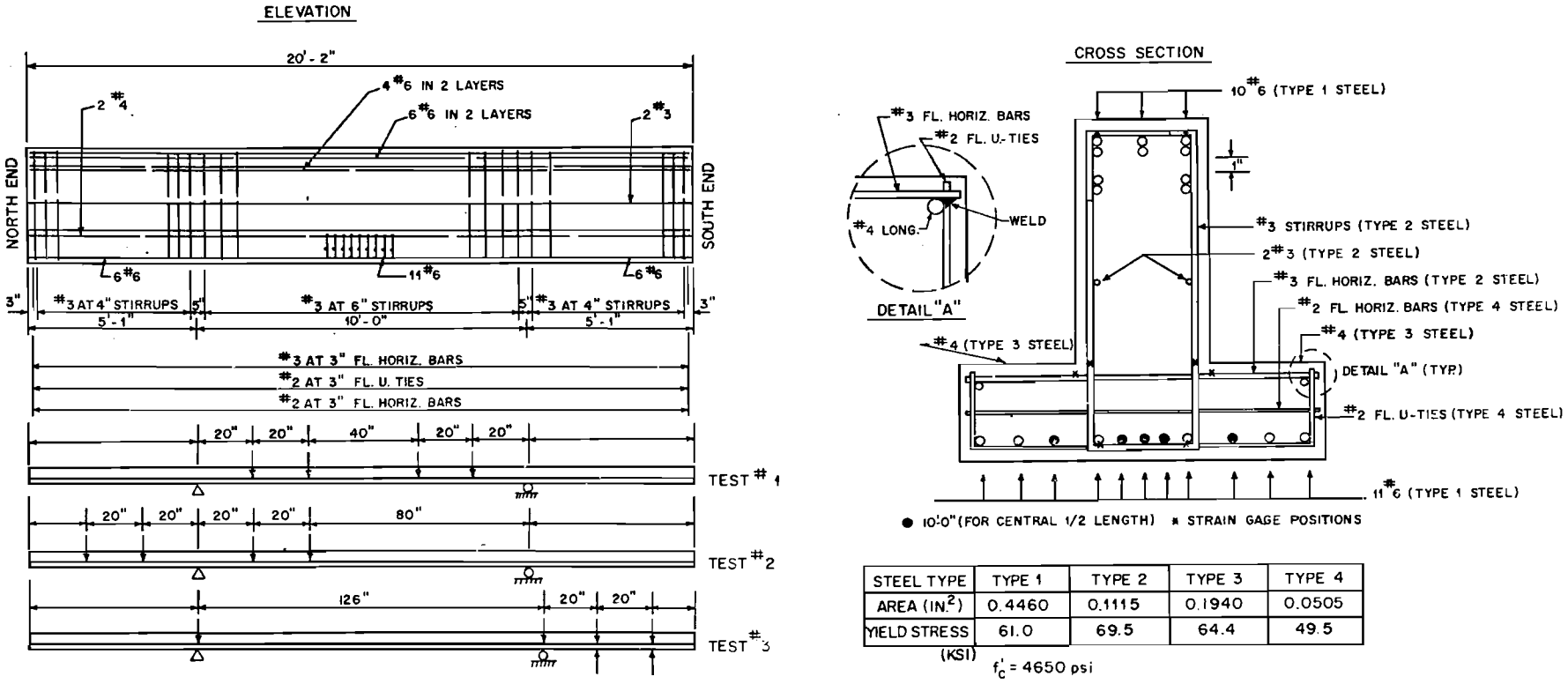

STEEL TYPE	TYPE 1	TYPE 2	TYPE 3	TYPE 4
AREA ($IN.^2$)	0.4460	0.1115	0.1940	0.0505
YIELD STRESS (KSI)	61.0	69.5	64.4	49.5

f'_c = 4650 psi

Fig. 2. Details of Specimen TC1.

flange reinforcing bars were welded to a #4 bar placed longitudinally at the upper corner of the flange. Test TC11 consisted of a positive moment test in which loads were applied between two supports. TC12 involved negative moment flexure at the portion shown as the left half of the specimen, and Test TC13 involved pure torsion applied at the portion shown as the right end of the specimen.

Specimen TC2, shown in Fig. 3, contains the same longitudinal reinforcement as that used for TC1. Some #3 stirrups were placed at 6 in. centers throughout the length of the specimen. In addition, some one-legged stirrups that hooked around longitudinal bars on only one side of the web were placed at 6 in. centers over one-fourth of the length of the specimen, and supplementary #3 full stirrups at 6 in. centers were placed in another fourth of the length of the specimen, such that the specimen contained #3 stirrups at 3 in. centers in some 5 ft. lengths. At the 5 ft. length of the south end of the specimen, #3 stirrups bent in a triangular pattern were placed between the #3 full stirrups. Five separate tests were conducted on specimen TC2. The first three tests involved positive moment flexure with nominal critical shear spans of 20 in., as indicated by the sketches shown with Fig. 3. Tests 4 and 5 on specimen TC2 involved negative moment flexure. Each test setup involved the same loading patterns applied to regions that contained different types of web reinforcement.

Specimen TP3 is described in Fig. 4. The specimen contained three sets of prestressing wires, two of which were located in the flange and one in the lower part of the web. The centroid of the prestress force was below the centroid of the cross section, in order to prestress the specimen for positive flexural loading. The shear reinforcement in the web consisted of a pair of #3 stirrups spaced 4-1/2 in. apart throughout most of the length of the specimen. At the south end, for a 3 ft. length, single stirrups were spaced 4-1/2 in. apart. Transverse reinforcement in the flange was the same as that used for specimens TC1 and TC2, except that the #2 bar at midheight of the flange was omitted. Specimen TP3 was subjected to three separate tests, the first involving

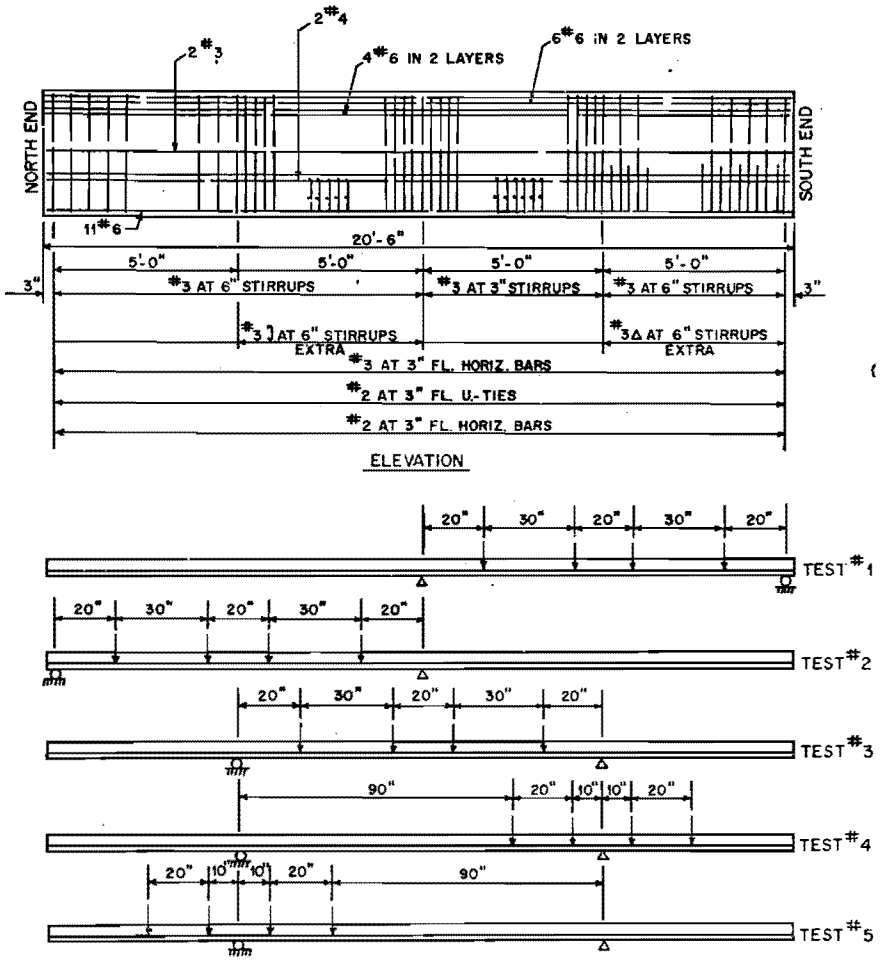

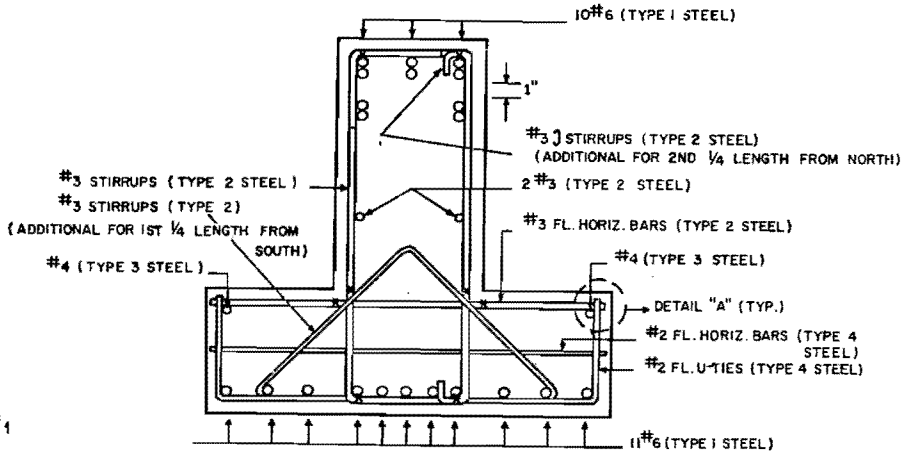

CROSS SECTION X POSITION OF STRAIN GAGES

STEEL TYPE	TYPE 1	TYPE 2	TYPE 3	TYPE 4
AREA (in^2)	0.4460	0.1115	0.1940	0.0505
YIELD STRESS (KSI)	61.0	69.5	64.4	49.5

f'_c = 4550 psi

Fig. 3. Details of Specimen TC2.

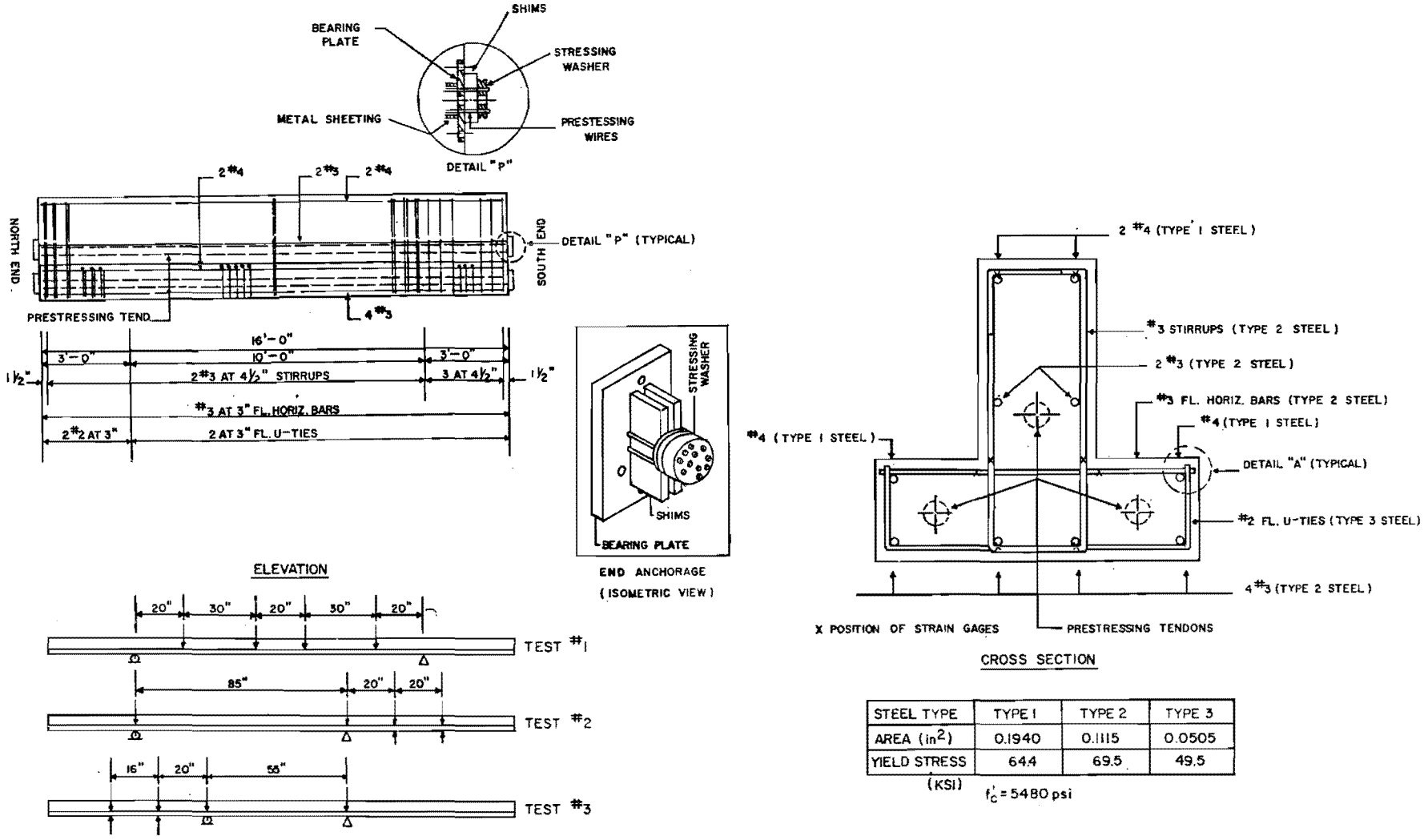

STEEL TYPE	TYPE 1	TYPE 2	TYPE 3
AREA (in^2)	0.1940	0.1115	0.0505
YIELD STRESS (KSI)	64.4	69.5	49.5

f'_c = 5480 psi

Fig. 4. Details of Specimen TP3.

positive flexural loading with torsion and the remaining two involving only pure torsion tests conducted in regions that had shown very little damage from the first two tests.

The details of specimen TP4 are shown in Fig. 5. Specimen TP4 was prestressed to resist negative moment flexure with the centroid of the prestressing force well above the centroid of the cross section. Supplementary longitudinal steel was provided at each corner of transverse web and flange reinforcement. The flange reinforcement for all prestressed concrete specimens was the same, consisting of a #3 bar across the top of the flange welded at its ends to the top of a #2 U-shaped bar and circling the remainder of the flange cross section. The welded hoops were placed at 3 in. centers throughout the length of each specimen. Web reinforcement consisted of #3 bars which were located at 3 in. centers through the north third of the length of the beam. The #3 stirrups were placed in pairs at 4 in. centers through the remaining two-thirds of the length of the specimen. Negative flexural loading plus torsion was applied to the south end of the specimen for Test 1, and the same pattern of loading was applied to the north end of the specimen for Test 2. The third setup, Test TP43, involved a pure torsional loading applied midway between clamped support regions located 35 in. each side of the centerline of the specimen.

The second specimen that was prestressed for positive moment flexural loading is illustrated as specimen TP5 in Fig. 6. The centroid of the prestressing force was located below the centroid of the cross section, and longitudinal steel identical to that used for specimen TP3 was augmented with supplementary longitudinal bars. The amount of longitudinal steel at the top of the web and at the bottom of the flange for specimen TP3 was doubled for specimen TP5. Transverse reinforcement in the flange was the same for each specimen. Shear reinforcement in the web of specimen TP5 consisted of #3 closed stirrups at 4-1/2 in. centers through the test region at the south end of the specimen, pairs of #3 stirrups at 4-1/2 in. centers through the center test region of the specimen, and pairs of stirrups at 9 in. centers in the test region at the

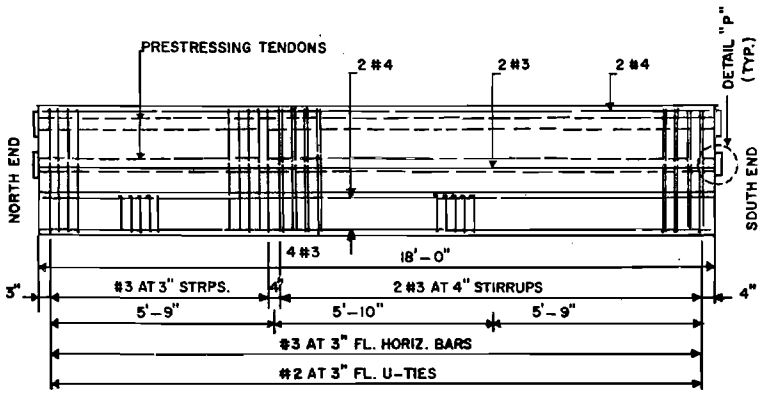

ELEVATION

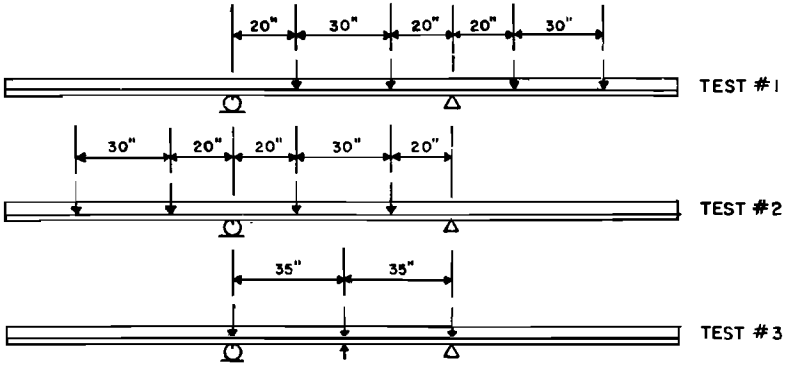

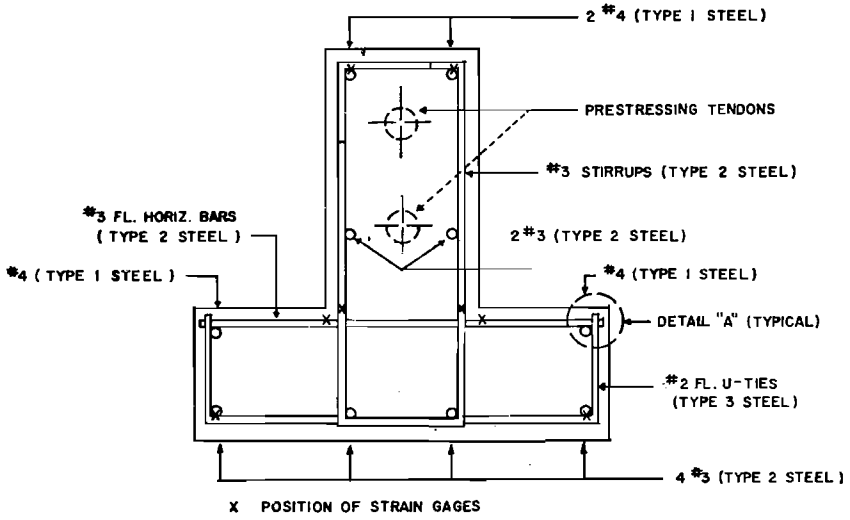

STEEL TYPE	TYPE 1	TYPE 2	TYPE 3
AREA ($in.^2$)	0.1995	0.1090	0.0481
YIELD STRESS (ksi)	68.2	70.6	52.0

f'_c = 5100 psi

Fig. 5. Details of Specimen TP4.

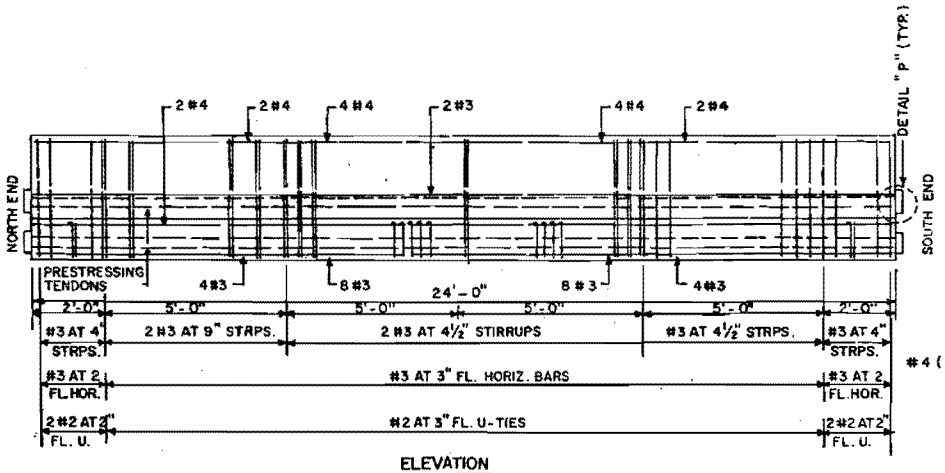

ELEVATION

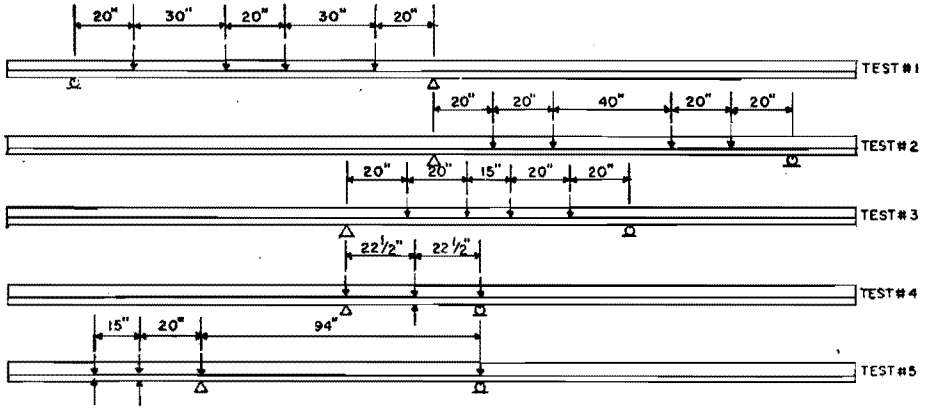

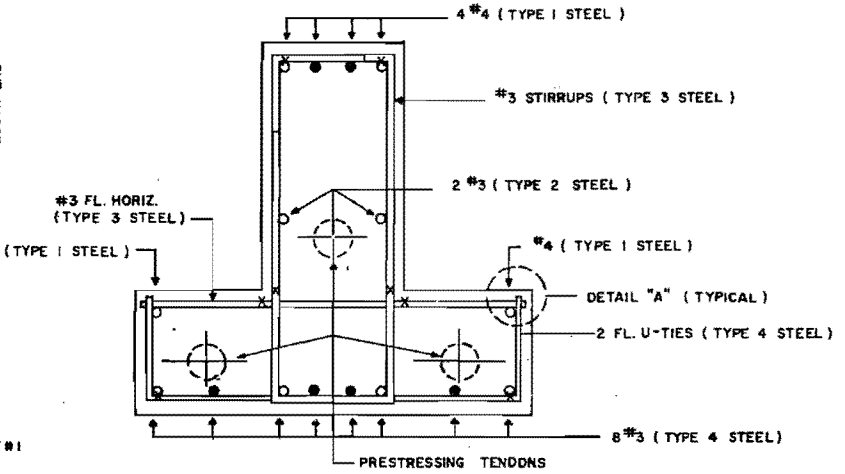

CROSS SECTION

STEEL TYPE	TYPE 1	TYPE 2	TYPE 3	TYPE 4
AREA (IN.^{2})	0.1920	0.1126	0.1090	0.0481
YIELD STRESS (KSI)	66.2	76.4	70.6	52.0

f'_c = 5530 psi

Fig. 6. Details of Specimen TP5.

north end of the specimen. Obviously, the variables of major interest for this specimen involved both the amount and the placement of stirrup reinforcement in the web. Positive moment flexural loading with torsion was applied to the north end of the specimen in Test 1 and to the south end of the specimen for Test 2. Test 2 employed a shorter shear span between supports and load points than did Test 1. Test 3 involved the same shear spans as Test 2 but employed a shorter distance between supports in order that the magnitude of bending moment would be smaller for Test 3 than for Test 2. Test 4 involved pure torsion applied 22-1/2 in. between clamped support regions, and Test 5 involved pure torque applied in a cantilevered torsion of the specimen near the north end. The length of specimen TP5 was made 50 percent greater than that of TP3. It was possible to perform five tests on the longer specimen compared with three tests on the 16 ft. length of specimen TP3.

The details of specimen TP6, the second specimen prestressed for negative moment flexural loading, are shown in Fig. 7. Specimen TP6 is 50 percent longer than specimen TP4, the first negative moment prestressed specimen. Longitudinal reinforcement and flange reinforcement for specimen TP6 were made identical to that employed for specimen TP4. Stirrup reinforcement for the web consisted of #3 closed stirrups at 4 in. centers in the north end test region and #3 stirrups at 2 in. centers through the central test region. Number 3 stirrups were spaced at 3 in. centers near the south end for a pure torsion test of that region. The first two tests of specimen TP6 involved negative moment flexural and torsional loading, and the final three tests involved pure torsional loadings.

Only deformed bar longitudinal reinforcement was used for specimen TC7, as indicated in the diagrams of Fig. 8. Longitudinal reinforcement was made the same as that used for specimen TC3, as was flange reinforcement for TC7. The spacing of #3 closed stirrups was made 4 in., 2 in., and 6 in. in 60-in. long test regions of the specimen. Test TC71 involved positive moment flexure and torsion. Test TC72 involved negative moment flexure and torsion, and Test TC73 involved pure torsion loading applied on a cantilevered portion at the south end of the specimen.

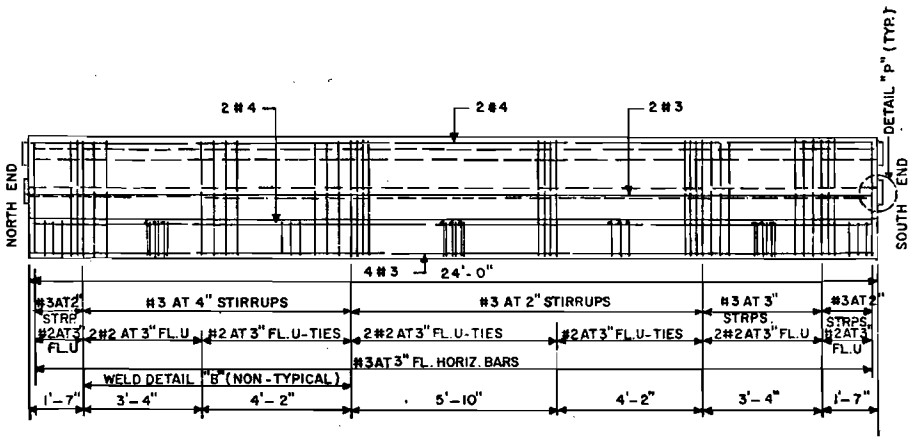

ELEVATION

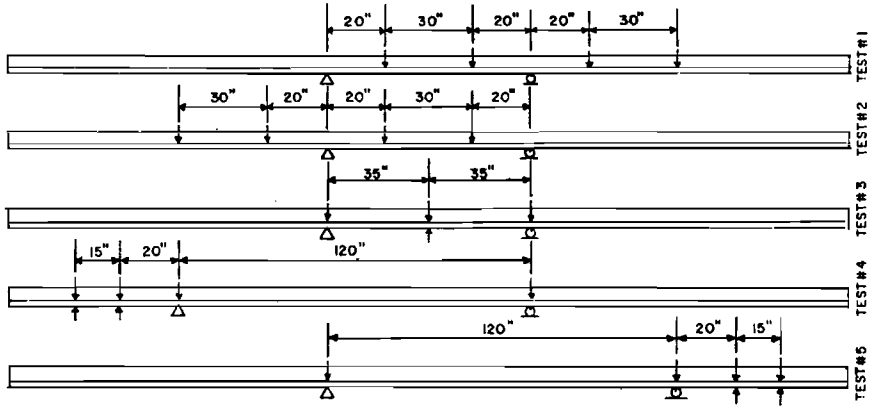

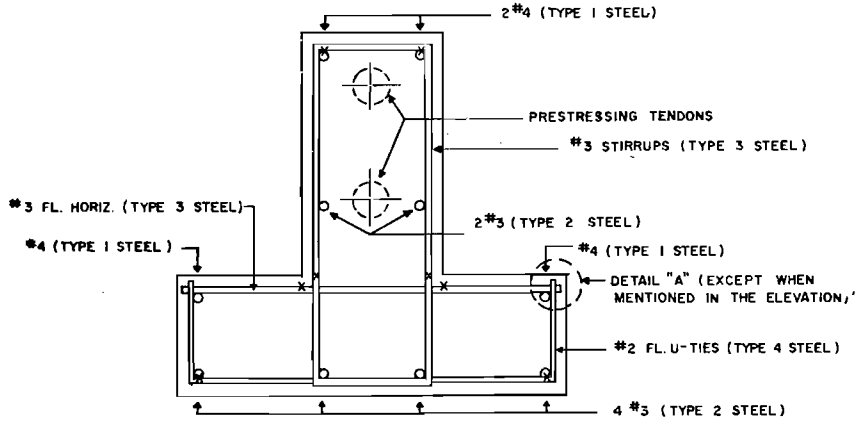

X POSITION OF STRAIN GAGES.

CROSS SECTION

STEEL TYPE	TYPE 1	TYPE 2	TYPE 3	TYPE 4
AREA ($IN.^2$)	0.1920	0.1126	0.1100	0.0481
YIELD STRESS (KSI)	66.2	76.4	71.8	52.0

f'_c = 5160 psi

Fig. 7. Details of Specimen TP6.

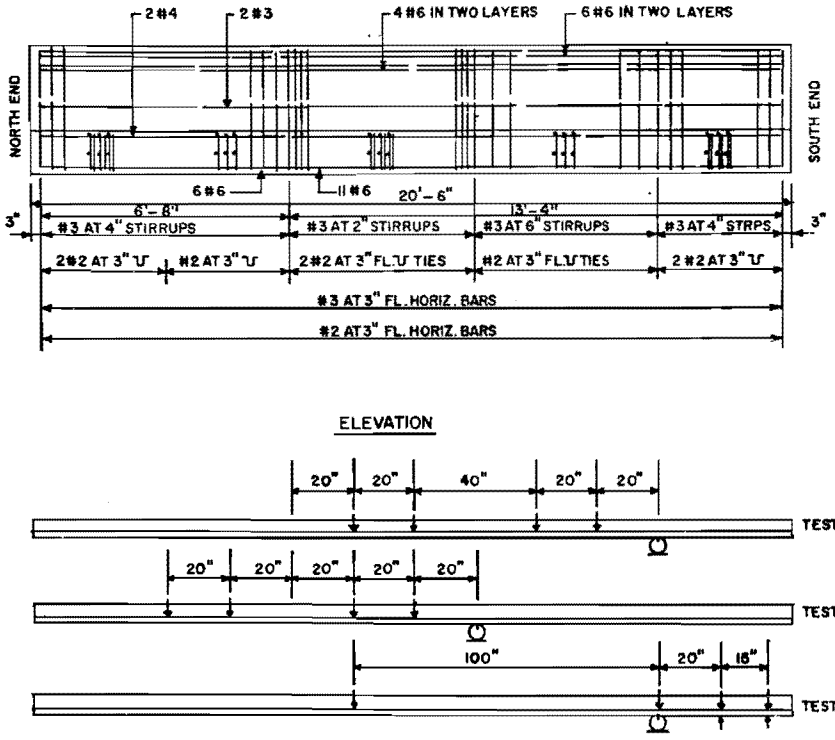

ELEVATION

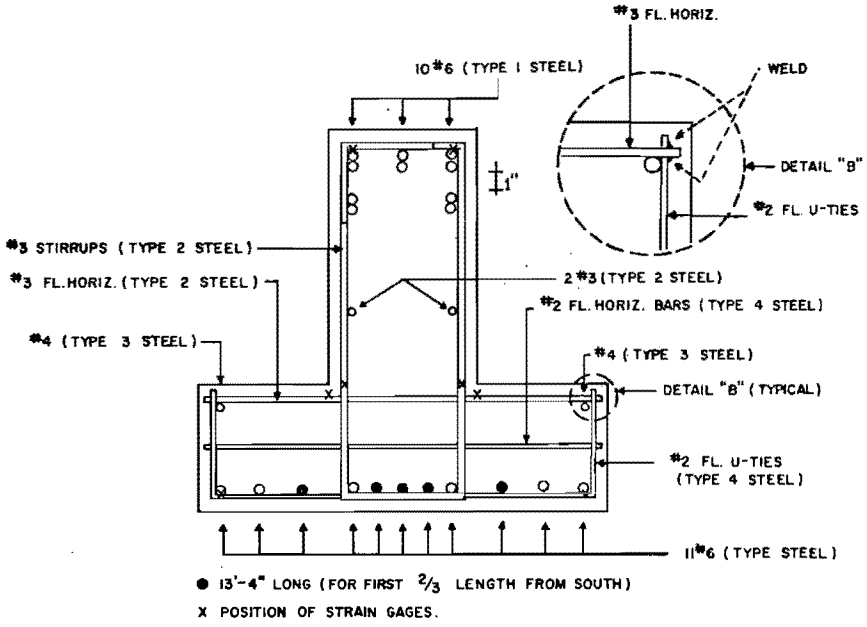

CROSS SECTION

STEEL TYPE	TYPE 1	TYPE 2	TYPE 3	TYPE 4
AREA (IN^2)	0.4460	0.1130	0.1995	0.0481
YIELD STRESS (KSI)	61.0	80.0	68.2	52.0

f'_c = 4560 psi

Fig. 8. Details of Specimen TC7.

All of the prestressed concrete specimens were post-tensioned and all of the prestressing wires were grouted. The oompression strength of control cylinders for all prestressed concrete specimens showed strengths f'_c somewhat higher than 5000 psi, but never greater than 5800 psi. The compression strength of control cylinders for reinforced concrete specimens reflected a strength varying from 4400 to 4800 psi. The average value of the strength of at least 5 and usually 9 cylinders per specimen is listed near the lower righthand corner of Figs. 2 through 8.

Concrete mixes were designed on the basis of Texas Highway Department specifications used for inverted T-beam bent caps. The model proportions at one-third scale employed a coarse aggregate with a maximum size of 3/8 in., thereby containing a smaller proportion of fine aggregate than that generally associated with a 3/8-in. maximum aggregate mix. It was considered significant to retain relative particle distribution in the one-third scale model specimens, and the laboratory mix presented no unusual problems of workability.

The yield strength of reinforcement used for test specimens was determined with test coupons cut from the same rods that were placed in the specimens. The strength of reinforcement used in each specimen is tabulated with details given in Figs. 2 through 8. Generally, the #6 bars had a yield strength of 61 ksi. The strength of #4 bars was somewhat higher, varying from 64.4 ksi to 68.2 ksi. The strength of #3 bars varied from 69.5 ksi upward to as much as 80 ksi. The #2 U-shaped ties indicated a yield strength near 50 ksi.

Prestressing tendons were made from 1/4 in. wire with a minimum tensile strength of 240 ksi, a nominal area of 0.0491 sq. in. and a modulus of elasticity near 29000 ksi. The tendons, prestressing hardware, and prestressing jacks were provided by the Prescon Corporation.

Loading and Support System

Specimens were supported during tests on concrete piers from the floor of the test laboratory. Supporting assemblies included bearing plates and a 3/4-in. diameter roller which extended beneath the entire

width of the flange at the point of support. A sketch of the support assembly detail is shown in Fig. 9. The location of reactions could be adjusted simply by moving the concrete bearing piers to desired locations along the length of the specimen.

Loads were applied through hydraulic jacks acting against load frames that straddled the test specimen. The loading frames were connected to anchor rails connected in turn to the laboratory floor. The anchor rails permitted movement of the test frames longitudinally for application of load to various regions of each specimen. Figure 10 contains photographs of the loading system in position for a positive moment plus torsion test. Figure 10(a) shows four load frames in position for loading between supports, one of which may be seen in the lower righthand corner of the picture. Hydraulic rams were reacted against load cells which in turn pushed against the load points on the flanges of the test specimen. Figures 10(b) and 10(c) show photographs of the hydraulic ram and load cells. A diagram of the assembly used between load cells and the test specimen is provided in Fig. 11. The assembly shows the use of a steel ball to concentrate the applied force at the center of a bearing plate on the flange of the test specimen. Loads could be monitored both by pressure gages in the hydraulic system and by readings from the load cells.

During every test, only two magnitudes of load were applied to the specimen at any instant. In all tests involving flexure plus torsion, one set of loads representing dead load was held constant while another set of loads was increased in order to represent various levels of live loads plus dead load. In many instances the dead loads were applied at four locations, and live loads were applied at four locations. In each case the four hydraulic rams for dead load would be operated through the same manifold and the four rams for live load plus dead load would be operated through a common manifold. Only two hydraulic pumps were used during any single test.

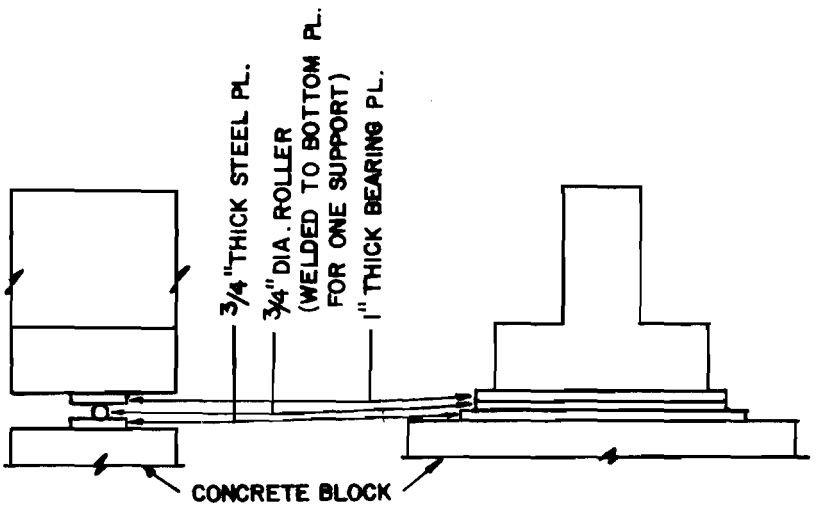

Fig. 9. Support assemblies.

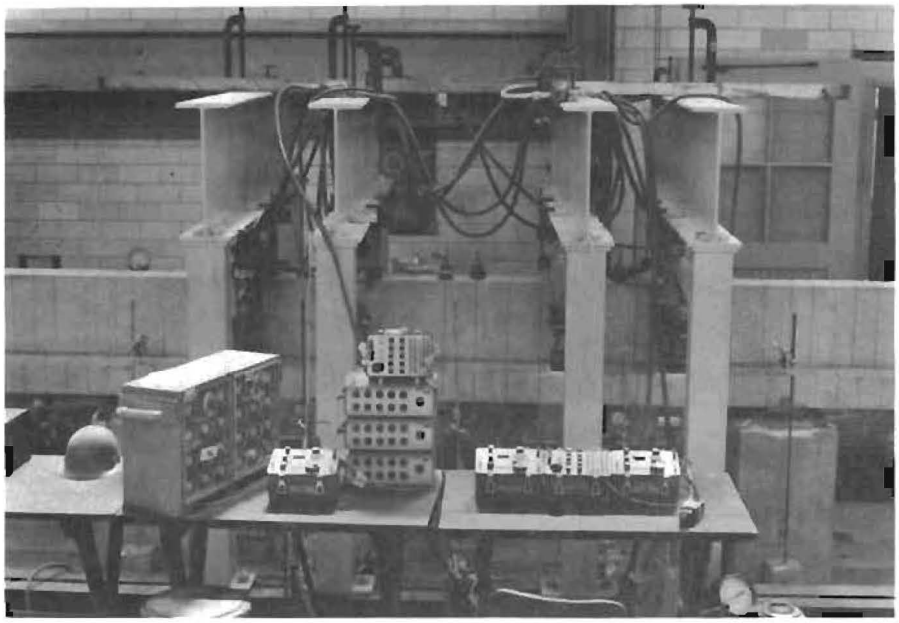

(a) Test setup for positive moment combined with torsion and shear.

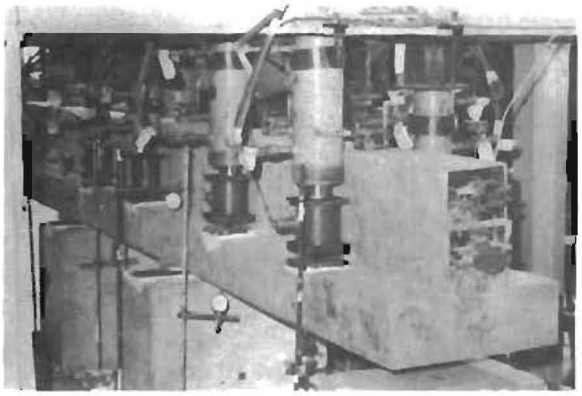

(b) Elevation.

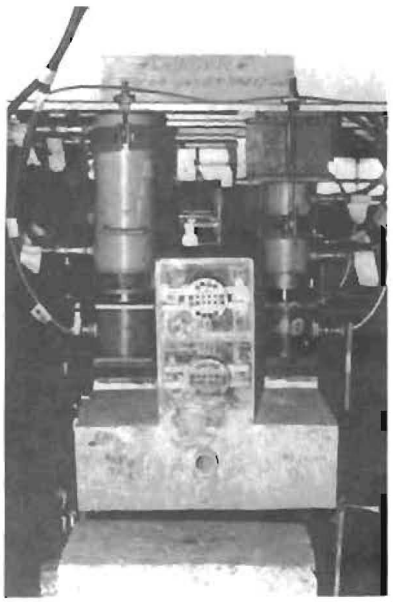

(c) End view.

Fig. 10. Typical load and support conditions.

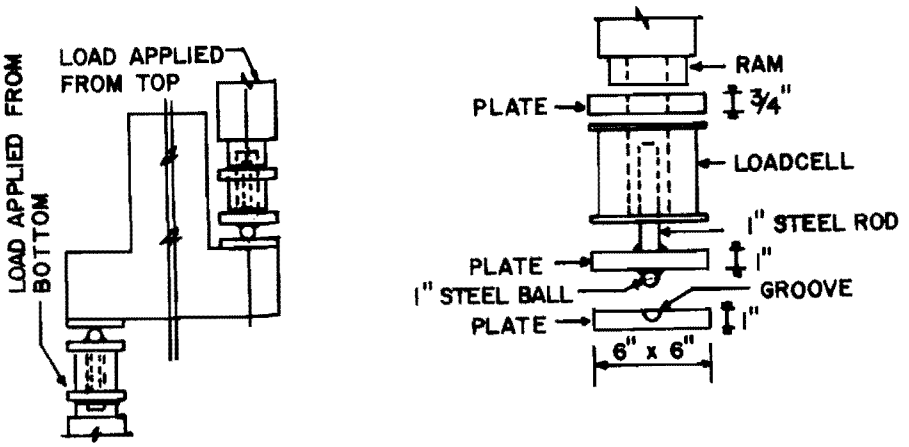

Fig. 11. Load assembly.

Instrumentation

Load Monitoring. Hydraulic pressure gages were attached to each of the two hydraulic systems used for the loading rams. The pressure gages could be read to the nearest 50 psi (500 lb. load), and the friction of packing within the rams could alter the effective application of force by as much as 500 lbs. Consequently, the loads could have been as much as 700 or 800 lbs. different from the value indicated by hydraulic pressure gages. The hydraulic monitoring system served two principal functions. Loads could be brought very close to desired magnitudes simply by pumping enough fluid to reach a desired pressure, and the availability of the pressure readings served as a back-up and a check on the alternate, more accurate load cell monitoring system.

Test loads were applied through load cells, as shown in Fig. 10(c). Most of the load cells had a capacity near 40 tons, with a gage factor for which 30 microinches of strain indicated approximately 1000 lbs. Strain meter readings in the order of 10 microinches are about as fine as one should attempt. Consequently, the load cell monitoring system should be accepted as accurate to the nearest 300 lbs. Model dead loads of 10 kips could have been 3 percent in error, and maximum loads near 50 kips would have been less than 1 percent in error.

Deflections. During each test, several different types of deflection readings were made. The vertical deflections in the plane of the web were of interest, and the twisting of the flanges out of their original unloaded plane were, of course, significant for the torsion study. In addition, the magnitude of rotation between support points and load points was measured.

Most of the deflections were monitored with dial indicators located near the reactions and near the points of loading. The dial indicators were placed under the flange on each side of the beam near each reaction. Additional dial indicators supported from the laboratory floor were placed beneath the flanges near the points of load and near the center of the web at the point of loading. Supplementary dial indicators

for the measurement of horizontal displacement were placed near the top of the beam against the face of the web.

The lateral displacement of the web between load points and support points was an indication of web twist. The magnitude of web twist both at support points and at load points was measured also with some inclinometers placed in convenient locations near supports and near load points. All of the inclinometers were mounted for reading along the top of the web. Inclinometers consisted of a bubble level and a calibration for maintaining the level of the bubble throughout a test. As the inclinometer is adjusted to maintain the level bubble, the change of inclination can be read with a calibrated leg used for the leveling.

Steel Strains. The distribution of load within reinforced concrete specimens can be traced partially, at least, by means of strain gages attached to the reinforcement of the specimen. Seventy to more than 100 strain gages were attached to reinforcement for each specimen. The strain gages for reinforcement were usually 1/4 in. gage length, foil strain gages. The gages were attached to the reinforcement with an epoxy, and a cushion and waterproofing were used to encase each gage after it had been attached.

Strain gages were attached to approximately 25 percent of the web stirrup reinforcement. Most of the strain gages on stirrups were placed at the same level as the top face of the flange. Longitudinal flexural steel received some strain gages, particularly those bars located in the extreme corners of the cross section. No attempt was made during a specific test to read all of the numerous strain gages on reinforcement. Only those gages nearest the test region were monitored for most of the tests.

Test Procedure

One of the objectives of the research was to observe the nature of cracks that might be expected under service load conditions that would involve torsion reversals as traffic crosses the bent cap. The test procedure for all tests involving a combination of flexure and

torsion began with several cycles during which live load was applied first to the flange on one side of the web and then to the flange on the other side of the web. Generally, in two stages of loading, all load points were subjected to the stringer dead load, nominally 10 kips on the laboratory specimen. Next, the concentrated loads were increased to 25 kips where live loads were assumed to be acting. Subsequently, the 25 kip loads were reduced to the dead load value of 10 kips and the opposite set of loading rams were increased to the 25 kip live load value. The specimen was examined at each stage of the loading to identify cracks that formed, and forces on selected stirrups were monitored from the strain gage readings. Once again the 25 kip loads were reduced to the 10 kip dead load value and forces on the opposite load points were increased to the live load value of 25 kips. The loading and unloading cycle was repeated at least one more time. If the deflection dials, strain gage readings, and crack distribution indicated insignificant change from the first or second cycle of loading, after the third cycle of live load the live load was not removed but was increased in gradual steps until failure occurred. The dead load of 10 kips per load point was maintained at all points not subjected to the live load.

The loading and reaction arrangement for a positive moment plus torque specimen is illustrated in Fig. 12(a). Figure 12(b) contains an illustration of a cantilever or negative moment plus torsion loading arrangement. Near the reaction to the overhang or cantilever region of a negative moment test, the magnitude of shear, flexure, and torsion is determinate, and the distribution of flexural moment, shear force, and torque is as illustrated in the diagrams of Fig. 12(b). Symbols that are shown with the moment diagram, shear diagram, and torque diagram consist of the distances a_1 and a_2 and the forces P and LL. The load, P, is the sum of two dead loads plus one live load at a stringer reaction. The load, LL, represents live loads.

Tests that involved positive moment flexure plus torque produced determinate flexural moments and flexural shears, but an indeterminate amount of torque at various portions of the span. Reactions to the beams

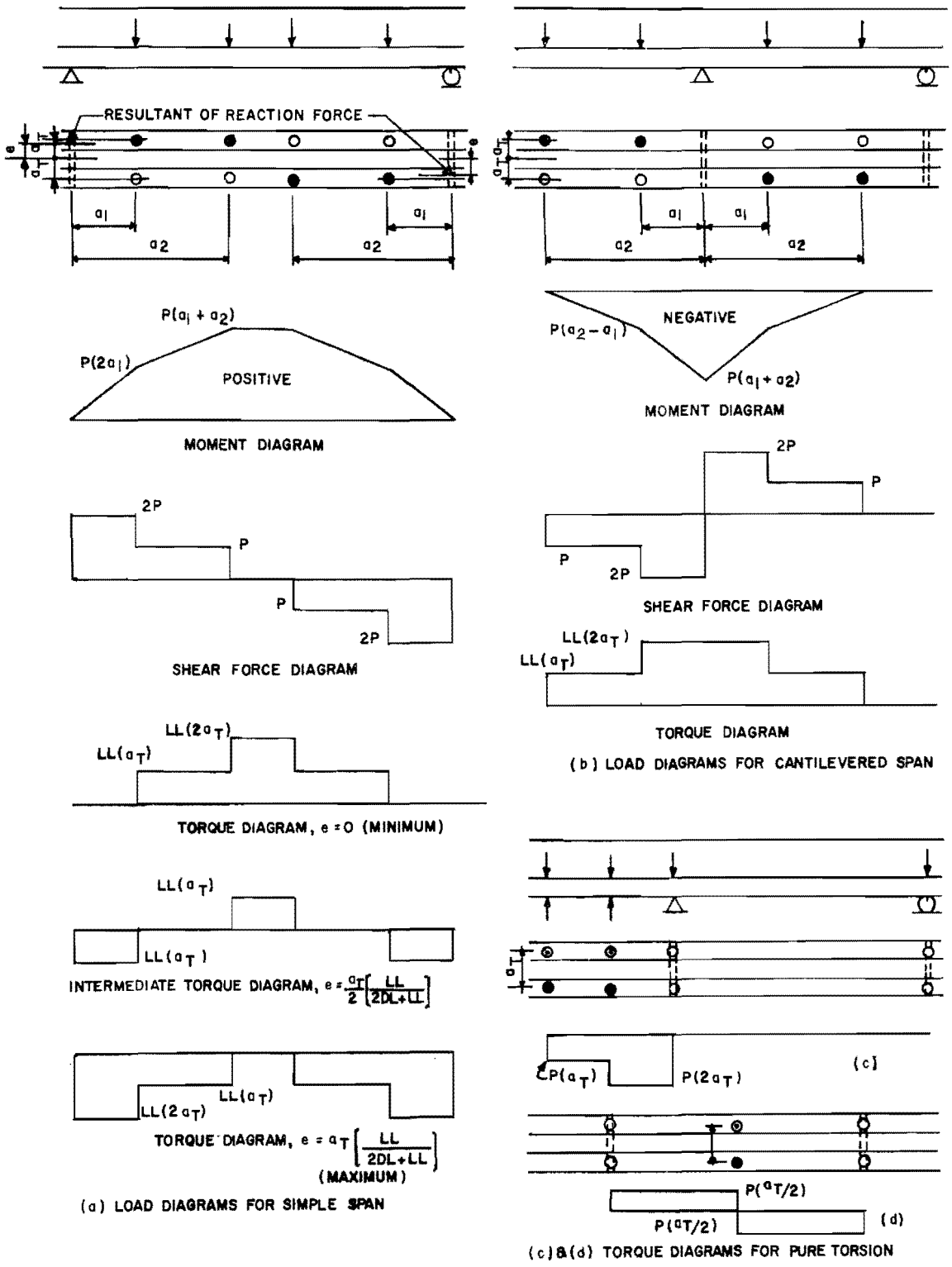

○ CONSTANT LOAD (CLAMPING LOAD FOR PURE TORQUE), P = 2DL+LL (APPLIED LOAD ON A BEARING SURFACE FOR PURE TORQUE)

● INCREASING LOAD

⊘ INCREASING LOAD APPLIED FROM BOTTOM

Fig. 12. Load diagrams.

could occur throughout the length of the rocker or roller placed beneath the flange. The centroid of a reaction, therefore, could occur at some eccentricity, e, from the centerline of the test beam, as indicated in the top sketch of Fig. 12(a). If the eccentricity were equal to zero, all torsion would be of the same algebraic sign and it would reach a maximum through the midsection. On the other hand, if the eccentricity were equal to the moment arm in the direction of the applied torsional force, the maximum torque would occur in the end regions of the specimen near the supports. It is more likely that an intermediate torque diagram actually occurs in which maximum torsions of opposite sign occur in the regions near the support and at midspan.

The loading arrangements for pure torsion tests are shown in Figs. 12(c) and 12(d). When pure torque was applied to a cantilever region, again the magnitude of torsion is determinate and the distribution of torque is illustrated in the diagram of Fig. 12(c). If torsion is applied between clamped supports, the specific magnitude of torque each side of the point of load application remains indeterminate. For the reduction of test data it was assumed that the pure torsion tests for span regions illustrated in Fig. 12(d) would be equal each side of the point at which torsion was applied. Loads were applied in steps until failure occurred for the pure torsion tests. No attempt was made to cycle pure torsion loads back and forth.

CHAPTER 3

SERVICE LOAD BEHAVIOR

Service Load Behavior of Reinforced Concrete Specimens

Analysis for Design. Stringer reactions that were assumed for design of the prototype bent cap girders were taken as 90 kips dead load and 120 kips of combined live load and impact. The typical spacing of stringers is 6 ft. to 8 ft. At one-third scale for the dimensions of the laboratory model, the stringer spacing should vary from 2 ft. to 3 ft. Loads require a scale factor of one-ninth, such that specimen loadings would be equal to 10 kips of dead load and 12 kips of live load. The nominal span-to-depth ratios for inverted T bent cap girders appear to be from 2 to 4 for cantilevered members, and 4 to 8 for spans supported at each end. Similar proportions were observed for the arrangement of test specimens.

The maximum spacing of stirrups for reinforced concrete specimens can be determined generally on the basis of stirrup action as hangers. The design ultimate load R for one stringer in accordance with AASHO Specifications[2] becomes

$$R = 1.3[D + \frac{5}{3}(L + I)] \qquad (3.1)$$

$$= 1.3[10 + \frac{5}{3}(12)]$$

$$= 39 \text{ kips for the laboratory specimens}$$

The hanger capacity within a stringer spacing ℓ_s should be as great as R. Thus

$$R \geq \frac{\ell_s}{s} A_v f_y \qquad (3.2)$$

using A_v = cross section area of one stirrup leg

f_y = yield strength of a stirrup

s = hanger spacing

In order to increase the probability of a shear or hanger failure in the test specimens, stirrup spacings, s, were made large enough for most specimens that the analytic or computed values of R were less than 39 kips. For example, the stirrups were spaced at 4 in. and at 6 in. apart in different test regions in specimen TC1 that used stringer locations 20 in. apart. The "nominal" values of R for the 4 in. spacing was 33 kips, but only 22 kips for the 6 in. spacing.

In the flanges transverse reinforcement was made large enough that local "bracket" weakness would not interfere with observations of combined flexure and torsion behavior for the overall specimen. In accordance with Eq. (11-29) of the ACI Building Code[3] and a design ultimate load R = 39 kips, the transverse flange reinforcement A_{vf} can be estimated as

$$A_{vf} = \frac{1}{64}\left[\frac{R}{6.5(1 - 0.5\,\frac{a}{d})\phi\sqrt{f'_c}} - b_e d\right] \qquad (3.3)$$

in which a = distance from face of web to center of bearing plate (a = 4 in. for all test specimens)

b_e = effective width of flange for each load R

A value of b_e equal to the width of bearing plus five times the distance "a" has been recommended.[1] It would give $b_e = 6 + 5 \times 4 = 26$ in., but with a stringer spacing of only 20 in. the b_e value must be reduced to 20 in. The amount of A_{vf} for the 7 in. thick flange (d = 6 in.) becomes 0.74 in.^{2} For all specimens, #3 bars were used at a spacing of 3 in. to provide at least $\frac{20}{3}(0.11) = 0.73$ in.^{2} of transverse reinforcement in the flange. In addition, all reinforced concrete specimens (TC1, TC2, and TC7) contained supplementary #2 bars 3 in. apart at midheight of the flange providing an additional 0.33 in.^{2} of steel for A_{vf}.

Longitudinal flexural reinforcement was proportioned such that none of the tension bars would yield under design ultimate loads. For example, the nominal tension stress (neglecting torsional effects)was 42 ksi for a positive design ultimate moment of 3120 k-in. on specimen TC1. Grade 60

bars were used. In the negative moment region subjected to the same moment of 3120 k-in. the nominal stress can be estimated (neglecting torque) also as 42 ksi.

Behavior under Repeated Cycles of Service Load. Specimens subjected to loading for flexure combined with torsion had eight points of loading representing eight stringer reactions. Dead loads of 10 kips were applied to all eight load points indicated by the open rectangles on the plan view diagram of a test region in Fig. 13(a). Loads of 15 kips, representing a 25 percent overload live load, were then added to four of the 10 kip dead loads indicated by the cross-hatched rectangles of Fig. 13(b). The 15 kip live loads will be referred to hereafter as live load, even though it should be understood that they represent a 25 percent overload above the nominal design live load plus impact.

The cycled torsional loading proceeded from the load condition shown in Fig. 13(b) to that shown in Fig. 13(a) as live loads were removed from the specimen, but dead loads were retained at all load points. The subsequent loading arrangement is shown in Fig. 13(c), with live loads applied at the cross-hatched rectangles opposite those indicated in Fig. 13(b). After all readings had been made and all visible cracking had been identified, the specimen once again was returned to the load condition illustrated in Fig. 13(a). One more complete cycle of load reversal was applied for each of the tests. Thus, the loading would consist of that shown in Fig. 13(b), followed by that in Fig. 13(a), followed by that shown in Fig. 13(c), and a return to the dead load condition illustrated in Fig. 13(a). If the deformed condition and reinforcement strain readings showed only small changes from the previous identical live load condition, live loads were increased at locations indicated by solid rectangles in Fig. 13(d) until failure took place. Live loads to failure were increased in increments between which a complete set of readings was made and the visible cracks were identified.

All of the reinforced concrete test specimens with stirrup spacings 4 in. or greater exhibited under the dead load condition some cracking on the face of the web very near the intersection of the flange. The cracks were horizontal (parallel to the flange) and visible only with

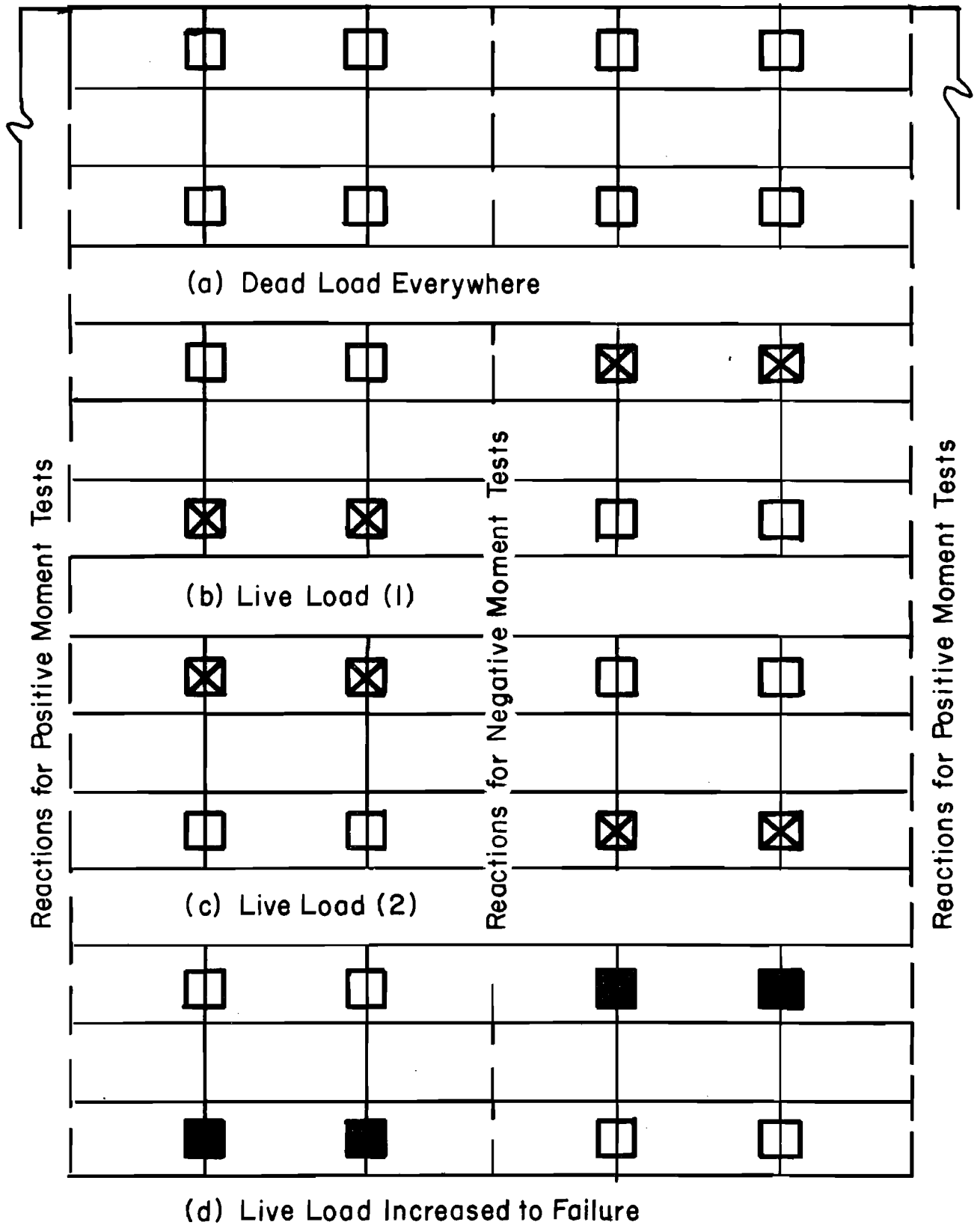

Fig. 13. Test load sequence.

bright light. Subsequent applications of the live load caused the initial cracks to widen and to extend. Strain gage readings indicated that the stirrups adjacent to applied live loads yielded in almost every case under the initial application of the live loads. In some instances yielding did not occur until after one cycle of live load application to the bearing plate on the opposite side of the web. Even after two full cycles of live load applications, stirrups located two or more spaces distant from the point of load applications exhibited low stress, and horizontal cracks did not propagate far from the bearing plates. In most cases the horizontal cracks at the corner between the face of the flange and the face of the web would propagate along the face of the flange diagonally away from the face of the web an inch or so each side of the bearing plate.

Very little flexural cracking was observed in any of the specimens during the first application of live load; however, some flexural cracking could be observed in all of the reinforced concrete specimens during the first cycle of live load plus dead load. Flexural cracks occurred in regions of maximum moment and each appeared first as a crack perpendicular to the longitudinal axis of the specimen and near the edge of the top face (negative flexure) or the edge of the bottom face (positive flexure) of the specimen. The cracks extended vertically along the face of the web or the face of the flange for an inch or more. Strain gages on the longitudinal reinforcement indicated that the maximum stress under repeated live loading was in the order of 25 ksi. If the influence of torsion on longitudinal stress in the steel is ignored, the nominal stresses in the flexural reinforcement would have reached 20 ksi theoretically. Flexural cracks that began on one side of the flange generally propagated entirely across the flange when the torsional reversal of live load was applied.

Transverse reinforcement in the top of the flange indicated that stresses as high as 15 to 18 ksi were developed under the service load condition. No flexural cracking specifically attributed to the tensile behavior of flange steel could be observed. Flexural cracking at the top of the flange was always influenced by the tensile cracking at hangers

near the corner of the intersection near the top of the flange and the face of the web. It is probable that the crack which appeared as a horizontal crack near the bottom portion of the web extended diagonally downward within the specimen toward the intersection of the vertical hanger and the flange reinforcement. Under service loading there was no evidence of distress or even high steel stress in the flange or in the flange reinforcement.

The service load performance of the test specimens as designed appear to be satisfactory in all respects, with the possible exception of the high stress observed in stirrups. However, even for the stirrups that yielded under the initial application of live load, subsequent applications of live load did not appear to generate higher strains in the once-yielded stirrups. The strains that were measured were not large enough to indicate significant strain hardening of the stirrups' steel. Apparently, the "rounded" characteristic of the stress-strain behavior of the steel in the initial inelastic stages of strain involved enough strain hardening to permit the reinforcement to stabilize under successive applications of "yield" strain under the service load condition.

Service Load Behavior of Prestressed Concrete Specimens

Analysis for Design. The response of prestressed concrete inverted T-beams to combined flexure and torsion represented the major undocumented phenomenon to be observed in this research. It was felt that the longitudinal precompression of the cross sections due to prestressing should improve both the flexural shear and bracket action by inhibiting or "delaying" the formation of tension cracking, thereby increasing the effective amount of shear force resisted by concrete alone. Therefore, the top transverse reinforcement used for the brackets was not changed, but the transverse #2 bars across midheight of the flange were omitted.

Among the four prestressed concrete specimens, seven different arrangements of #3 stirrups were employed. The tests of reinforced concrete specimens TC1 and TC2 had indicated that even though hangers had

been assigned for about half the design ultimate load, their ultimate capacity was adequate to develop the full ultimate load. Cracks in the web near the top of the flange had been quite obvious with the wide-spaced, single hangers at both 4 in. and 6 in. centers under the service loads. Among the various stirrup arrangements used for the prestressed specimens, the least amount of hanger capacity consisted of #3 stirrups 4.5 in. apart. The greatest amount of hanger capacity was provided by placing single stirrups 2 in. apart. On the basis of Eq. (3.2), the nominal capacity of hangers to support test loads R applied at each bearing plate can be estimated. The estimated values of R for Grade 60 stirrups are tabulated for prestressed concrete specimens in Table 3.1.

TABLE 3.1. NOMINAL HANGER CAPACITY FOR PRESTRESSED CONCRETE SPECIMENS

Specimen Test Region	Hanger Arrangement	Stringer Spacing, ℓ_s (in.)	Computed R (kips)
TP61	#3 @ 2"	30	99
TP41	pairs @ 4"	30	99
TP31	pairs @ 4.5"	30	88
TP53	pairs @ 4.5"	20	59
TP42	#3 @ 3"	30	66
TP62	#3 @ 4"	30	50
TP51	pairs @ 9"	30	44
TP52	#3 @ 4.5"	20	29

In order to observe whether some supplementary closed stirrups in the flange could improve torsional strength, the number of #2 U-shaped bars was doubled by placing in TP62 pairs of bars at the same spacing that had been used for single bars for other test regions.

Flexural reinforcement for prestressed concrete specimens was made adequate only to resist nominal ultimate test loads and to satisfy nominal requirements for service load flexural stress without torsion. The

"light" flexural prestressing was used in order that for test observations the influence of torsion on longitudinal stresses, cracking, and compression capacity would be more readily apparent. The geometric properties of the specimen cross section based only on dimensions of concrete are illustrated in Fig. 14(a). Positive moment stresses after prestressing and at design moments (neglecting possible loss of prestress) are shown in Fig. 14(b). Again, neglecting possible losses of prestress, the stress conditions for negative moment specimens after prestressing and under design moments are illustrated in Fig. 14(c).

The allowable service load positive moment value of 1630 k-in. is governed by the limit of $0.4f'_c$ compression stress at the top of the web. It can be generated with the load arrangement for specimens TP31 and TP51 with eight dead loads of 10 kips plus four live loads of only 4 kips applied at each line of loads. The load arrangement for TP52 and TP53 requires 7 kips of live load at each line of loads to reach the 1630 k-in. moment. Consequently, the allowable positive moment compression stress was exceeded during the cycled "service" load test conditions. The ultimate moment flexural capacity of TP3 was estimated to be 3500 k-in., which is just adequate for the 49 kip flexural forces created by eight ultimate dead loads of 13 kips plus four ultimate live loads of 26 kips. Ultimate flexural capacity for TP5 was increased to 4000 k-in. by the addition of extra Grade 60 deformed bars in the top of the web and the bottom of the flange.

The allowable service load negative moment value of 2320 k-in. also is governed by the stress limit at the top of the web. Negative moment adequate to develop tension stress as great as $6\sqrt{f'_c}$ can be generated by eight dead loads arranged as shown for all negative moment test regions plus live loads of 13 kips applied at each of the four lines of loads (Figs. 5 and 7). Thus, for negative moment tests, the permissible stress condition for service loading was exceeded only slightly by the cycled live loads of 15 kips during each test. The computed ultimate moment capacity of 3770 k-in. of negative moments was adequate for 54 kips of live load along each load line. A test load of 54 kips would involve

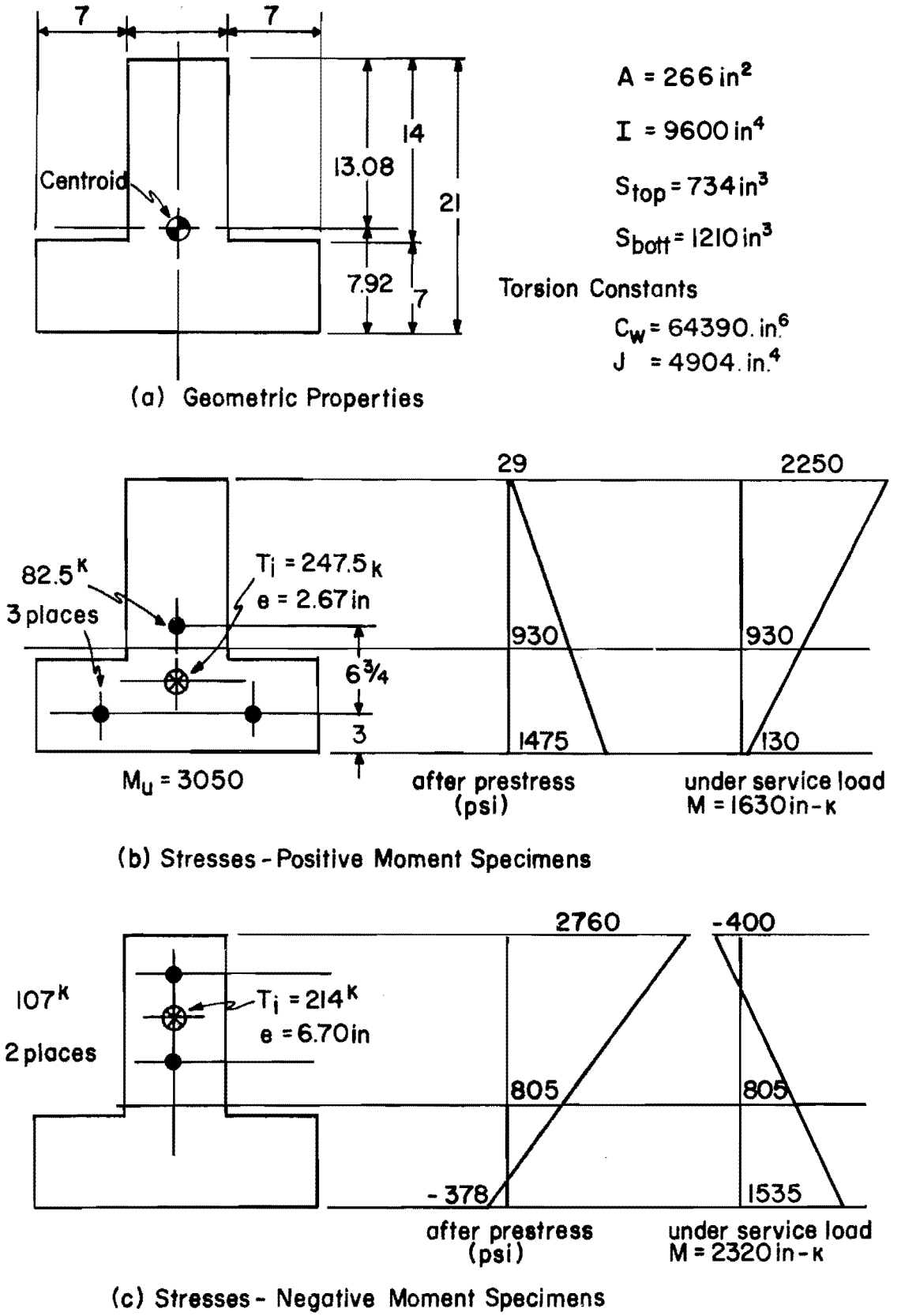

Fig. 14. Prestressed concrete stress analysis.

two dead loads of 13 kips plus one live load of 28 kips. The 28 kip live load is only slightly higher than the required 26 kip ultimate live load assumed for the testing program.

The prestressed concrete specimens were designed for probable failures in the web as a combination of flexural and torsional stresses reach the capacity of the compressed concrete. In contrast to the reinforced concrete specimens, most test regions contained an intentional excess of stirrup reinforcement in the web.

Behavior under Repeated Cycles of Service Load. The prestressing operations were conducted in accordance with instructions from the Prescon Corporation, whose prestressing hardware and equipment were used, and strain readings were made from strain gages attached to longitudinal bars in the top corners and along the bottom corners of each specimen. The strain gage readings indicated that prestressing actually applied to specimen TP3 and specimen TP6 corresponded very closely to the theoretical or desired magnitude and location of force. The same type of strain gage readings for specimen TP4 indicated that the magnitude of prestressing force actually applied was about 15 percent less than the force assumed for the design of the specimen. The prestressing force actually applied to specimen TP5 appeared to be about 12 percent smaller than that which was assumed for the design.

Load tests of specimens TP3 and TP5 involved positive moment plus torsion. When the specimens were loaded initially with dead load at all eight load points no cracks were observed on the surface of the specimens. After the torsional live loads had been applied, a flexure-type crack could be observed near the bottom corner of the specimen beneath the two live load support points nearest midspan. Strain gages on the bars in each corner indicate that the tension surface strain was 500 microin. per in. at the time first cracking was observed. After the test live loads had been removed from one set of load points and reapplied to the opposite set of load points, the initial flexural cracks closed and new cracks appeared beneath the live load support points nearest midspan. Recycling

of the live load revealed few new cracks, but the initial cracks were observed to "join together," extending in some cases completely across the bottom face of the specimen. After the service load cracking had occurred, recycling of the live loads created very little change in the cracks that could be seen nor in the magnitude of strains indicated on the longitudinal reinforcement.

No cracks appeared at the face of the web near the top of the flange (indicating hanger tension) under service loads that were applied to the positive moment test specimens. It should be recalled that the amount of stirrup reinforcement in specimen TP3 and test region TP51 was approximately double that used for the reinforced concrete specimens. Even though the stirrup spacing for TP52 was the same as that which permitted some yielding under service loading on reinforced concrete specimens, there was no evidence of overstress on the prestressed concrete member. Strain gage readings showed that the maximum hanger stress under cycled live loads reached only 12 ksi. Strain gages on stirrups adjacent to points of applied live load indicated that the maximum stress in all other stirrups under service load conditions remained less than 10 ksi.

Strain gages attached to transverse bars along the top of the flange indicated some service load stresses as high as 24 ksi. Cracks associated with such stresses were very difficult to observe as they had to occur in the corner between the face of the flange and the top of the web. Without the evidence that was obtained from strain gages on the reinforcement, it would have been impossible to tell whether cracks in that corner should be attributed to hanger tension or transverse flexure at the top of the flange.

Specimens TP4 and TP6 were subjected to negative moments combined with torsion. No cracking, either flexural, torsional, hanger, or top of flange flexure, could be seen under service load conditions applied to specimen TP4. The level of initial prestress in the top of the negative moment specimens generated precompression strains near 500 microin. per in. The application of dead loads of 10 kips plus two live loads of 12.5 kips

caused approximately 800 microin. per in. change in strain in the top fibers. The net change from 500 microin. per in. of compression strain to 300 microin. per in. of tension strain did not create enough tension strain to crack the concrete. In the same manner as that observed for the positive moment specimens, there were enough stirrups to sustain hanger loads without revealing tension cracks along the face of the web. Transverse flexural steel along the top of each flange likewise restrained the formation of tensile cracks along the top of the flange. One had the impression as the tests progressed that the precompression of the stem near the top of the flange tended to restrain the formation of cracks in the web. Strain gages on stirrups and on transverse bars as well as strain gages on longitudinal steel tended to verify the absence of tensile strains high enough to create cracks visible to the eye.

The absence and delay of initial crack formation in prestressed concrete inverted T-beams made their apparent performance under service load seem superior to that of inverted T-beams reinforced only with deformed bars. The prestressed concrete specimens behaved in a more stable manner with smaller variations than the corresponding reinforced concrete specimens had exhibited in response to the alternate cycles of live load. Flexural cracks occurred only at the higher loads, and they were less visible in the prestressed concrete specimens. The removal of live load permitted the precompression to close flexural cracks. The comparison of prestressed concrete and ordinary reinforced concrete specimen behavior in the tests that were performed is not altogether fair in that the prestressed concrete specimens contained considerably more stirrup reinforcement than that which was used in the reinforced concrete specimens. The test procedure and the level of test loading for service load conditions revealed no ill effect from the intentional underdesign of prestressed concrete specimens in flexure.

Strain gages that had been attached to the longitudinal steel tended to encourage the impression that prestressed concrete specimens behaved monolithically under the influence of combined flexure and torsion at least until service load levels had been reached. The lack of

prominent cracking and the low level of strains that were measured under service loadings should be associated with uncracked, homogeneous, and isotropic behavior in the prestressed concrete specimens. Service load analysis of the prestressed concrete, therefore, could be based on relationships for an elastic continuum. In contrast, the behavior of ordinary reinforced concrete specimens involved cracking so extensive that the overall member should be considered analytically as an assemblage of fractured mechanisms even at service load levels of response.

Serviceability Criteria for Hanger Performance

Even though all arrangements of hangers (stirrups) supported the nominal ultimate loads, some yielding of hangers was observed under nominal service loads. The force in any specific hanger is a function of applied load, base plate size, and some "effective distribution zone" that incorporates hangers nearest the applied load. A relationship between the force in one leg of a hanger $A_v f_s/2$, hanger spacing s, applied load $P_D + P_L$, base plate width B, cantilever load position "a" from face of support, and an unknown effective width coefficient γ, can be expressed

$$A_v f_s \left(\frac{B + \gamma a}{s}\right) = (P_D + P_L)2 \tag{3.4}$$

Data from all torsion-plus-moment tests listed in Table 3.2 contain values of γ for f_s equal to the yield strength of hangers and $(P_D + P_L)$ values corresponding to the measured load at first observed hanger yielding. The values of γ varied from a low of 1.6 with 2-in. stirrup spacing to a high of 6.1 with 6-in. stirrup spacing. The average of all values computed was 3.5.

As a serviceability control, it seems desirable to limit the hanger stress to values less than $2/3 f_y$ under service load conditions. The coefficient was taken as 3.0 to represent somewhat less than the average for all measured values, and Eq. (3.4) can be modified to serve as a serviceability control.

$$\frac{A_v}{s} = \frac{3(P_D + P_L)}{f_y(B + 3a)} \tag{3.5}$$

TABLE 3.2. HANGER YIELD LOAD ANALYSIS

Test No.	Hanger Yield Load (k)	Stirrup f_y (ksi)	Stirrup Spacing (in.)	γ
TC11	25	64.4	6	4.3
TC21	25	69.5	6	3.9
TC22	25	69.5	6	3.9
TC23	35	69.5	3	1.9
TC71	25	68.2	6	4.0
TP51	40	70.6	4.5	4.9
TP52	40	70.6	4.5	4.9
TP53	55	70.6	2.25	2.8
TC12	25	64.4	6	4.6
TC24	17.5	69.5	6	1.9
TC25	35	69.5	6	6.1
TC72	30	68.2	4	2.9
TP41	45	70.6	2	1.6
TP42	42.5	70.6	3	3.0
TP61	50	71.8	2	1.9
TP62	40	71.8	4	4.1
Average				3.5
Median				3.9

CHAPTER 4

STRENGTH OBSERVATIONS AND ANALYSIS

Failure Modes

The strength of concrete inverted T-beams is only as great as the weakest of several possible components or combinations of components that participate in the retention of applied loads. The components will be defined in terms of failure mechanisms or failure modes. Six failure modes were identified from the 27 tests that were performed. Among the 27 tests very few involved failures easily attributable to only one component, but failure generally took place after weakness was apparent in more than one failure mode. The strength of the entire cross section of a speciman can be interpreted in terms of resistance to flexure, flexural shear, or torsion, and any of the three will be reached only if there exists adequate local strength for hangers, flange shear, and flange bracket response.

Sketches of typical crack patterns for each mode of failure are provided in Figs. 15 through 20. Each mode is described in the following paragraphs:

(1) A cross section is considered to have failed in flexure when its resistance to flexural deformation ceases to increase and begins to decrease. Under the application of large flexural deformations, reinforcing bars and prestressing strand tend to yield or stretch without a reduction in tensile force. Simultaneously, the resistance of concrete and compressive reinforcement can remain relatively constant, but the amount of compressive "yielding" is limited by the amount of stress that can be redistributed by concrete before the concrete cracks and spalls at the surface of maximum compression strain. A flexural mode of failure is apparent when rather thin, flat particles of concrete appear to separate

from (spall) the face of maximum compressive strain. The sketches of Fig. 15 suggest characteristic cracking associated with flexural failure.

(2) Flexural shear failure for specimens with an effective shear span as short as that employed for these tests involves the yielding of all stirrups that cross a large crack that extends diagonally along the side faces of the web until the shear strength or compressive strength of uncracked concrete is exhausted. The maximum shear span near supports for any specimen test was only 18 percent greater than the effective depth of the member. The sketches of Fig. 16 indicate surface cracking of concrete associated with a flexural shear failure.

(3) The failure of "cross sections" in torsion involves a section that cannot be considered simply as a plane section perpendicular to the longitudinal axis of the member. Evidence of torsional distress in reinforced concrete or in prestressed concrete beams appears in diagonal cracks that extend in a spiral pattern from one face of a member to an adjacent face. Also, an apparent twisting along the overall length of the member occurs only under torsional loading. Failure begins in the form of diagonal tension cracks across which both longitudinal steel and stirrup reinforcement must transmit the tensile forces that were lost where the concrete cracked. As torsional force and deformation increase, the diagonal cracks extend in length and in width until reinforcement across the crack yields. If the anchorage strength of bars is not lost due to edge cracking, torsional deformation continues until there are one or more compression failures along the face nearest the center of torsional rotation. The diagram on Fig. 17 displays a set of forces that could act on a broken section of an inverted T-beam prior to a torsion failure.

(4) Hanger failure of stirrups is revealed by the vertical separation that occurs between the flange and the web at the top of the flange. The separation begins as a local phenomenon near the stringer bearing plate, but as the stirrups closest to the bearing yield the flange deflects and causes more hangers to share the concentrated stringer load. The sketch of Fig. 18 indicates that failure will occur only after all available

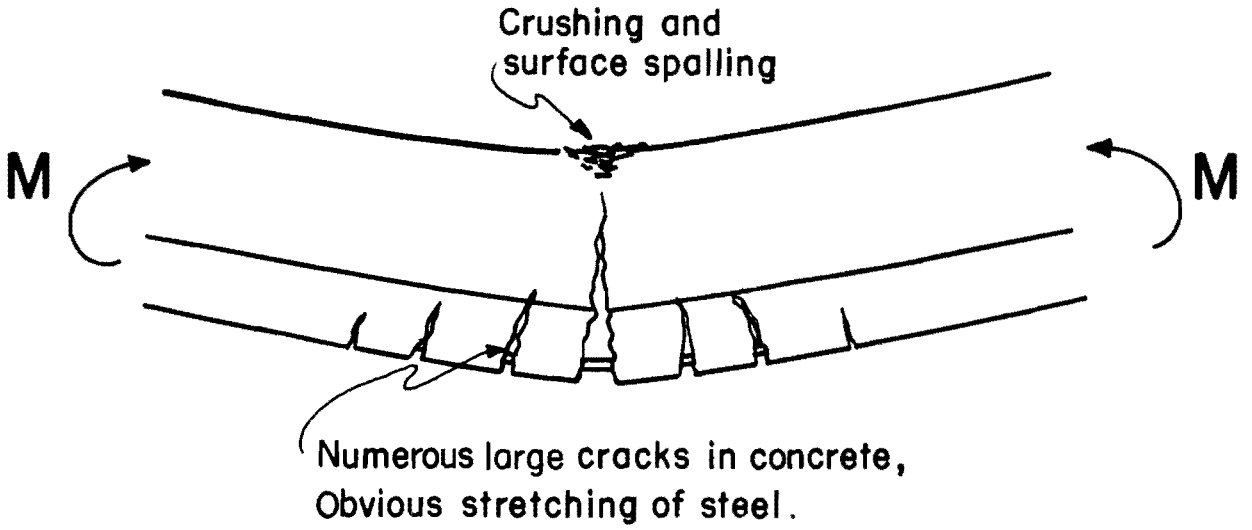

(a) FLEXURAL FAILURE - POSITIVE MOMENT

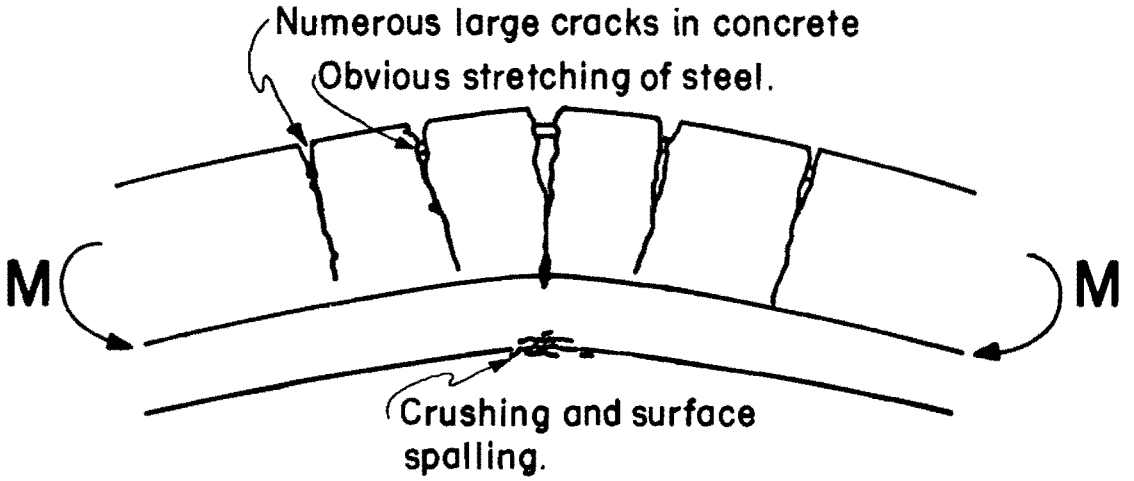

(b) FLEXURAL FAILURE - NEGATIVE MOMENT.

Steel stretches and concrete cracks become larger. Failure occurs only after compressive resistance is exhausted as revealed by spalling or flaking on the compressive surface.

Fig. 15. Flexural failure mode.

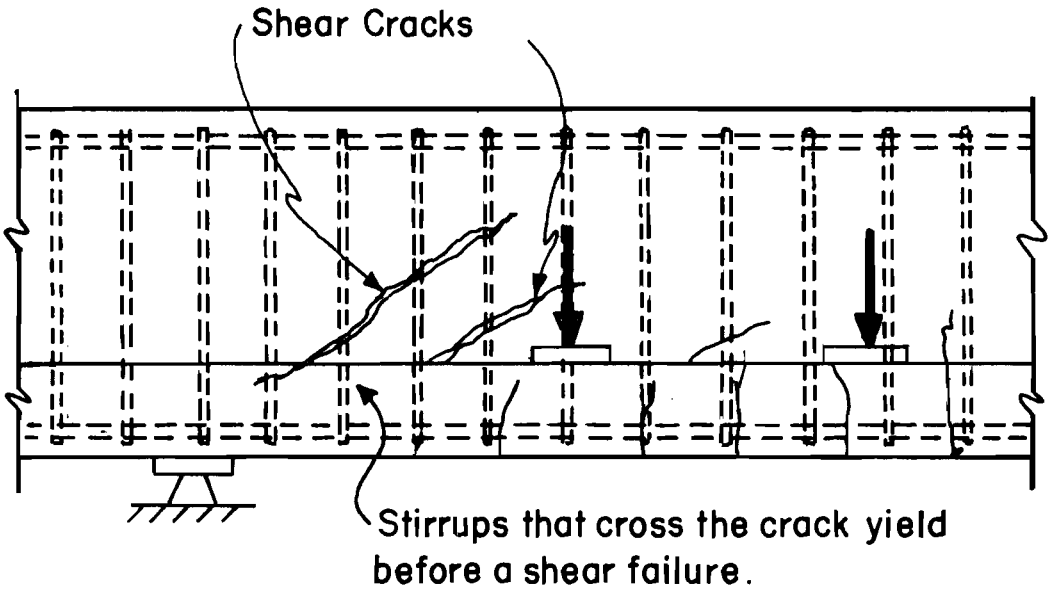

Fig. 16. Flexural shear failure mode.

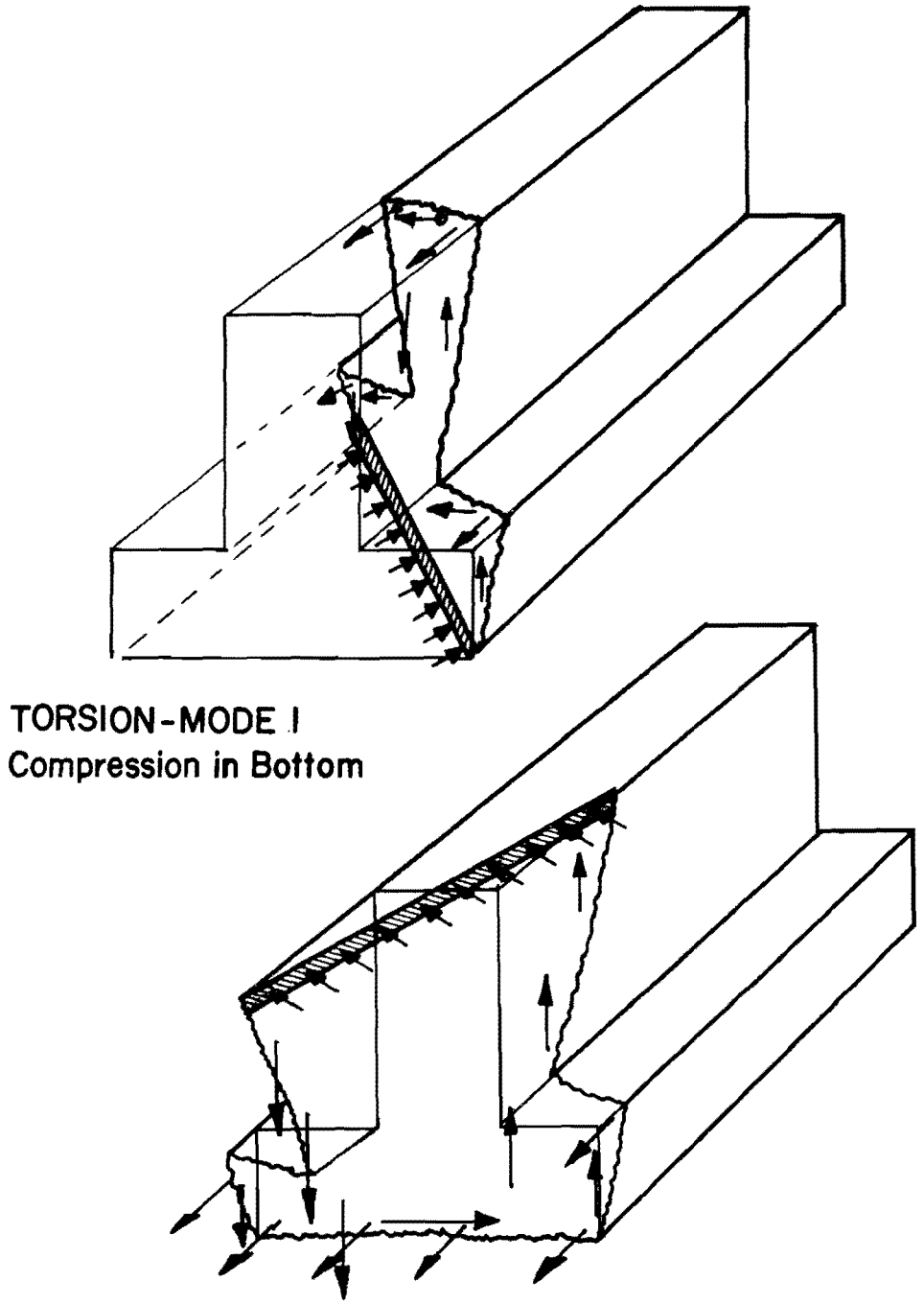

Fig. 17. Torsion failure modes.

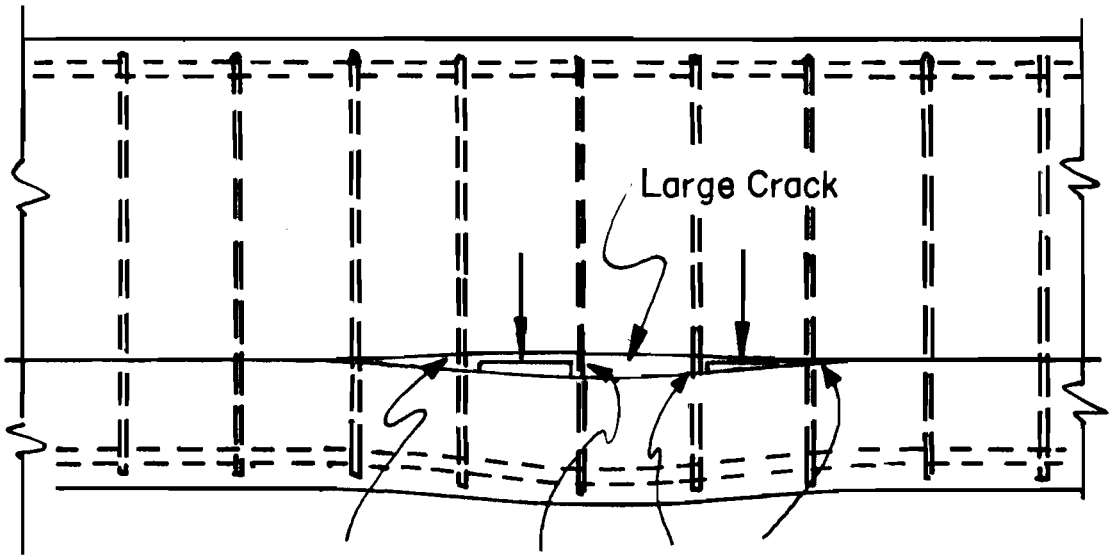

Fig. 18. Hanger failure mode.

stirrups have yielded unless the flange itself fails while trying to distribute longitudinally the stringer force.

(5) Flange shear or punching failure can take place if stringer forces are large enough to "punch out" the truncated pyramid of concrete beneath a bearing pad, as suggested in Fig. 19. Flange shear distress is most evident from the appearance of diagonal cracks emanating from the edges of the bearing plate. As is characteristic for concrete "shear" failures, the phenomenon of punching shear is actually another form of diagonal tension failure in the concrete.

(6) The strength limit referred to as bracket failure is used here to identify a local loss of resistance to load because the flange, acting as a bracket, tends to deform outward and away from the web while also deforming downward from loss of shear strength along the face of the web. The sketch of Fig. 20 indicates that bracket failure involves yielding of transverse bars acting in flexure across the top of the web. As the transverse bars yield, the "shear friction" force along the face of the web (or along the line of stirrup legs in this case) cannot be increased, and sliding may commence.

Test Results and Classification of Failure

A summary of test results is given in Table 4.1. The table displays for each test the recorded load at which stirrups reached yield stress, the load at which cracks opened to as much as 0.025 in., and the ultimate load that could be applied. The spacing of #3 web stirrups is given, and in the righthand columns, the letter code indicates the most prominent mode of failure. Ultimate load was taken as the maximum force that could be resisted by the test specimen. With the exception of punching and bracket-type failures, the specimens exhibited considerable reserve strength after the maximum load was attained. The reserve strength could be realized only after the development of wide cracks as internal resistances were redistributed to less damaged regions of a specimen. The local and sudden failure associated with punching and bracket shear precluded any capability for redistribution.

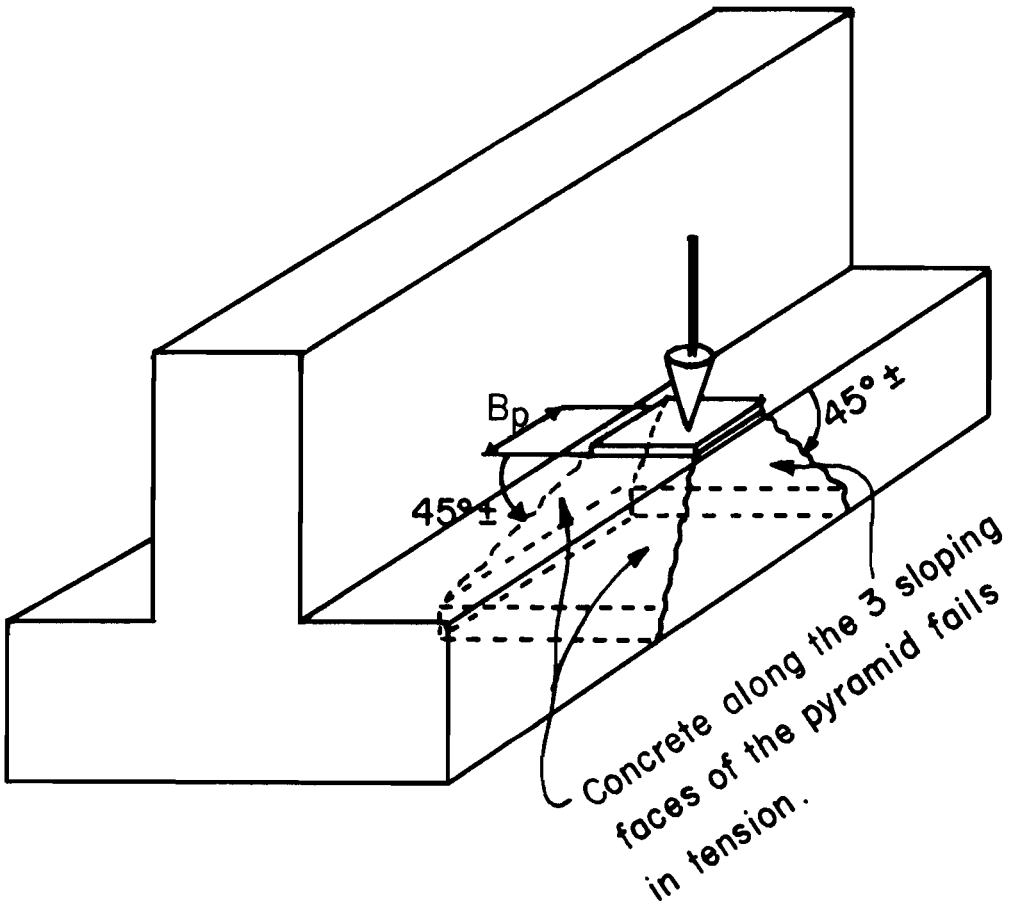

Fig. 19. Flange shear or punching failure mode.

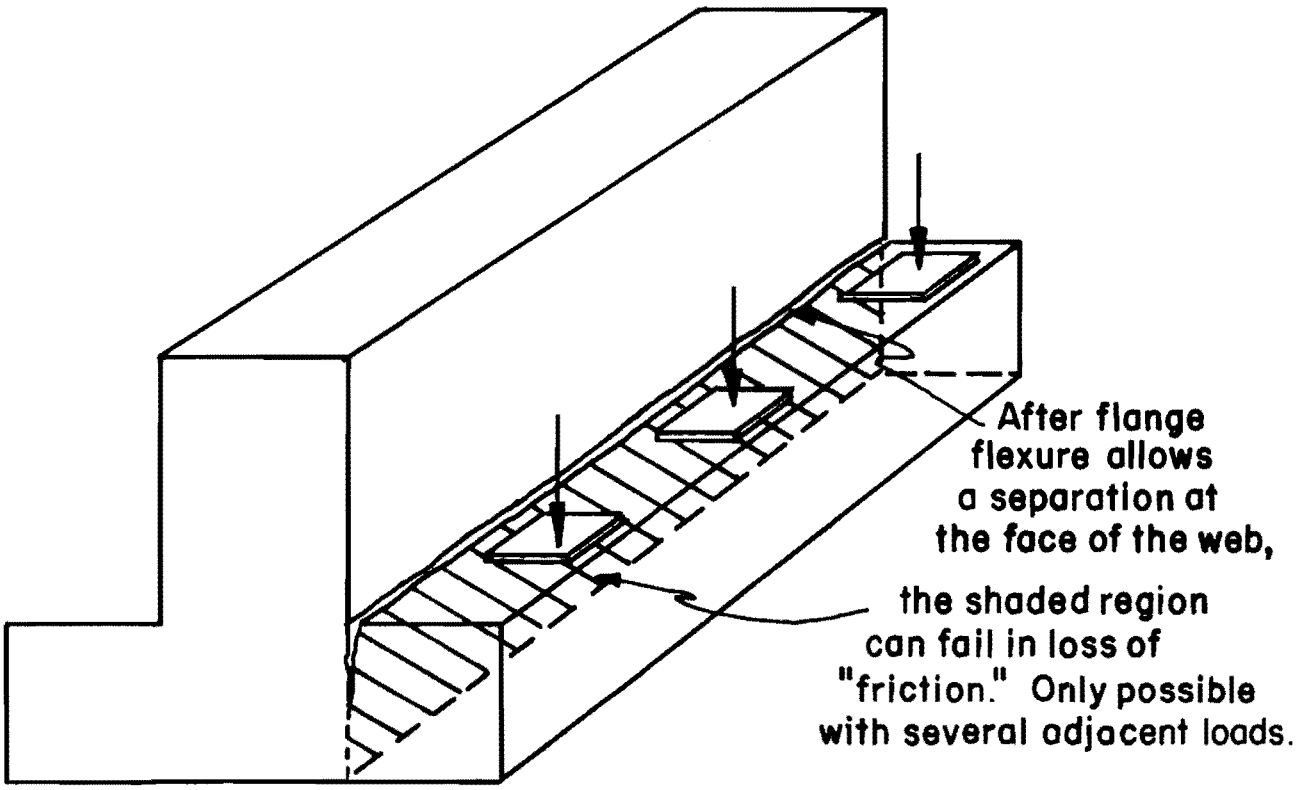

Fig. 20. Bracket failure mode.

TABLE 4.1. STRENGTH RESULTS

Test No.	Yield Load	Wide Crack Load	Ultimate Load	Stirrup Spacing	Failure Mode (See Code Below)
		Torsion plus Positive Moment			
TC11	25.0	35.0	39.0	6"	H
TC21	25.0	37.5	52.5	6"+extra #3Δ	T,S
TC22	25.0	37.5	47.5	6"	H
TC23	25.0	No Record	57.5	3"	P
TC71	25.0	35.0	52.5	6"	H
TP31	45.0[L]	30.0	52.0	4.5"	T,F,P
TP51	40.0	No Record	55.0	pairs @ 9"	H
TP52	45.0	45.0	52.0	4.5"	H
TP53	55.0	52.5	57.0	pairs @ 4.5"	T,S,F,B
		Torsion plus Negative Moment			
TC12	25.0	35.0	39.0	6"	T,S,F
TC24	17.5	30.0	55.0	6"+extra #3Δ	H,P
TC25	35.0	25.0	55.0	6"	H
TC72	35.0	35.0	52.5	4"	T,S,F
TP41	50.0	17.5	50.0	pairs @ 4"	P
TP42	42.5	45.0	52.5	3"	H,P
TP61	50.0	50.0	55.0	2"	P
TP62	45.0	40.0	50.0	4"	T,S,F
		Pure Torsion			
TC13	25.0	20.0	32.5	6"	T
TC73	25.0	20.0	32.3	4"	T
TP32	No Record	25.0	38.8	pairs @ 4.5"	T
TP33	32.0	30.0	34.0	pairs @ 4.5"	T
TP43	No Record	No Record	78.4	pairs @ 4"	H,P,B
TP54	No Yield	No Record	95.0	pairs @ 4.5"	T,S
TP55	No Record	25.0	30.0	pairs @ 9"	T
TP63	No Record	No Record	81.0	#3 @ 2"	P
TP64	30.0	32.5	34.2	#3 @ 4"	T
TP65	30.0	No Record	33.0	#3 @ 3"	T

[L]Yield of longitudinal steel preceded stirrup yield. Extra #3Δ ties were placed at bottom of web.

Failure Code: F = flexural failure
S = flexural shear failure
T = torsion failure
H = hanger failure
P = punching failure
B = bracket failure

The ultimate loads shown in Table 4.1 were applied at four bearing points for all of the torsion plus flexure tests. As the ultimate loads were being applied to the four bearing plates, an additional set of 10 kip loads was maintained constant on four bearing plates at the opposite side of the web from each live load bearing plate. The position of test loads was described with Fig. 13 of Chapter 3. Loads for pure torsion tests were applied in equal amounts to the top of a flange on one side of the web and the bottom side of the flange on the opposite side of the web.

In all of the tests, including those that were in regions intentionally underdesigned, the nominal ultimate load of 39 kips was supported. The nominal ultimate load was taken as 1.3 dead load of 10 kips plus 2.17 live load and impact forces of 12 kips.

Analysis of Hanger Strength. The mechanism of load retention in hangers can be analyzed on the basis of forces illustrated in Fig. 21(a). The flange region of an inverted T-beam can be considered as cracked away from the upper portion of the web after several passes of traffic with alternate applications of live loads on opposite sides of the web. The "effective hanger distance," x_h, represents the length of flange that can be considered capable of distributing the concentrated load longitudinally among hangers located at a spacing, s, along the web. As stirrups nearest to the applied load reach their yield stress, the force in each reaches its maximum value and remains constant for all larger strains. Increases in load simply extend the size of the crack as yielded stirrups stretch and the nearby stirrups pick up the extra load.

When live load is applied only on one side of a flange, there is a tendency for the loaded side of the flange to pry against the unloaded side and to overload stirrups nearest the live load, as indicated in Fig. 21(b). Again, after the stirrups nearest the load yield the "prying" force is distributed longitudinally by the flange until more stirrups are brought to their yield stress. The flanges of inverted T-beam bent caps are sufficiently stiff that at longitudinal distances more than a flange width away from the live load stirrups on both sides of the web resist approximately equal amounts of vertical force. Consequently, the

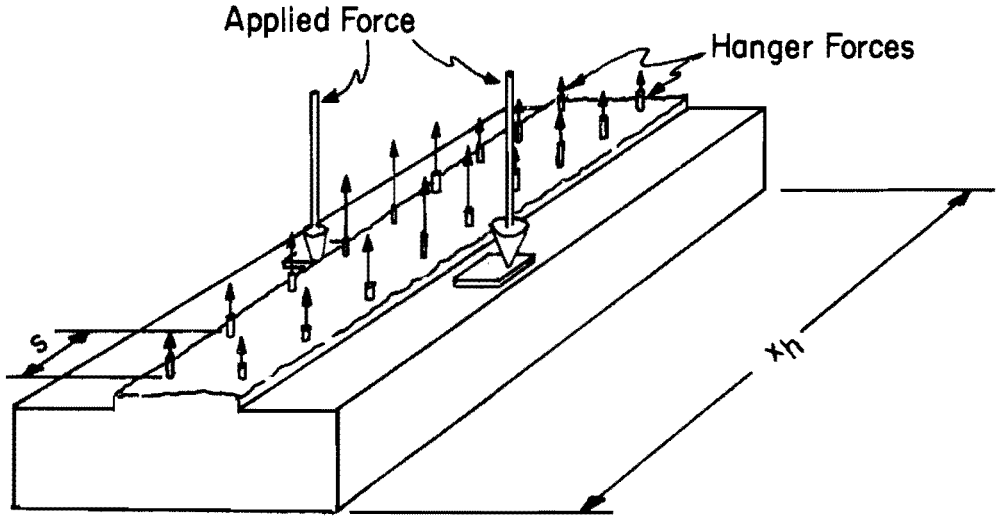

(a) Flange Loads and Hanger Forces

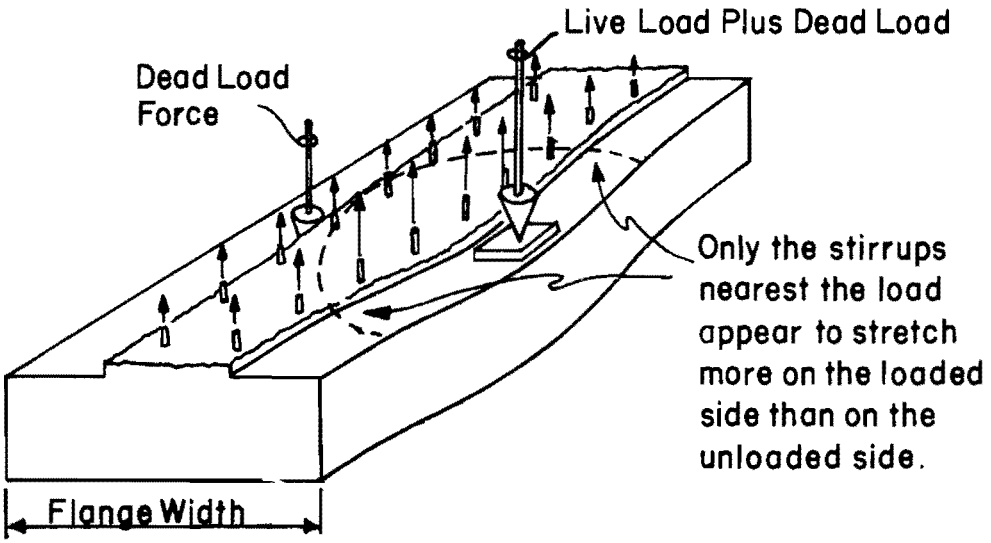

(b) Live Load applied on only one flange

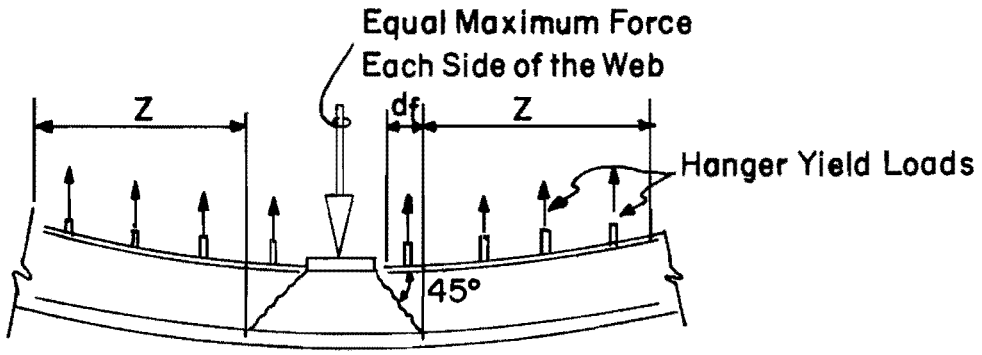

(c) Ultimate Load Near a Bearing

Fig. 21. Hanger forces in response to flange loads.

most severe load condition for hangers at ultimate load exists when both sides of the web resist maximum live load simulatneously, as shown in the illustration of Fig. 21(a).

The longitudinal distance x_h over which the flange forces can be distributed will be limited either by the longitudinal center-to-center spacing S of applied forces or by the capacity of the flange to distribute the applied force among the hangers. Flange capacity to distribute hanger forces will be limited by the shear capacity of the concrete in the flange either side of a bearing plate, as suggested by the sketch of Fig. 21(c). For the usual proportions of inverted T-beam bent caps there is always more flexural strength than shear strength in flanges, even for members that are prestressed to resist negative moment.

The shear capacity of a flange can be estimated as the ultimate stress $2\sqrt{f'_c}$ acting on the area of the flange $b_f d_f$. The accumulated hanger load within a distance z each side of a bearing plate is simply the sum of hanger yield forces $f_y A_v$ within the distance z. Shear capacity of the flange must exceed accumulated hanger loads, or

$$b_f d_f \, 2\sqrt{f'_c} \geq \frac{z}{s} f_y A_v \qquad (4.1a)$$

Rearranging:

$$z < \frac{2\sqrt{f'_c}}{A_v f_y} \, b_f d_f s \qquad (4.1b)$$

The effective length x_h for determining hanger capacity can be expressed as the sum of the bearing plate width B plus a distance $(z + d_f)$ each side of the bearing plate. Then with a stringer spacing S,

$$x_h \leq B + 2(d_f + z) \leq S$$

$$x_h \leq B + 2d_f\left(1 + 2\sqrt{f'_c}\, b_f \frac{s}{A_v f_y}\right) \leq S \qquad (4.1c)$$

The #3 hangers that were used for the tests reported here had values of f_y = 70 ksi, and specimen proportions gave b_f = 22 in., B = 6 in., A_v = 0.22 sq. in., with an average f'_c = 4600 psi. For these tests

$$x_h \leq 6 + 2d_f(1 + 0.194s) \leq S \qquad (4.1d)$$

Values of S varied among the different test regions.

Hanger capacity for a concentrated load P_h on one side of the web can be expressed as the strength of all stirrups within the space x_h or S, whichever is smaller. Then either

$$P_h = 4\sqrt{f'_c}\, b_f d_f + \frac{A_v f_y}{s}\left(\frac{B}{2} + d_f\right) \qquad (4.2a)$$

or

$$P_h = \frac{1}{2}\frac{A_v f_y}{s} S \qquad (4.2b)$$

The smaller value must be used.

The strength results that were listed in Table 4.1 included six failures that were attributed to hanger failure. In addition, hanger weakness was felt to be significant for the failure of three other test regions. The measured strengths for each of the nine tests are compared with results from Eq. (4.2a) or Eq. (4.2b), as listed in Table 4.2. Results from four tests listed in Ref. 1 involved no precracking of test regions prior to the sequence of loads that caused failure. Since all test regions involved only two ultimate loads per flange, whenever x_h exceeded S an effective value for x_h was taken as the average of x_h and S.

The ratios between calculated and measured ultimate loads are shown in the righthand column of Table 4.2. The majority of ratios is less than unity and the amount is significantly lower for the results from Ref. 1. There were four ratios greater than unity, each test involving some punching shear weakness or another failure mode that probably contributed to apparent hanger weakness. The ratios for predominantly hanger type failures appear to be very safe for design.

Design applications require the use of a capacity reduction factor φ when the Load Factor Method is used.[2] A rearrangement of the strength relationships of Eq. (4.2a) and (4.2b) makes the use of φ both convenient and obvious. The rearrangement provides minimum values for the design

TABLE 4.2. OBSERVATION AND ANALYSIS OF HANGER FAILURES

Test No.	Stringer Spacing S in.	Hanger Spacing s in.	x_h Eq. (4.1d) in.	Effective x_h in.	P_h Eqs. (4.2) kips	P_{ult} Observed kips	Ratio $\frac{P_h}{P_{ult}}$
TC11	20	6	27.6	28.8	37.0	39.0	0.95
TC22	30	6	32.0	31.0	39.8	47.5	0.84
TC71	20	3	25.0	22.5	57.8	52.5	1.10
TC25	20	3	25.0	22.5	57.8	55.0	1.05
TP51	30	2@9	28.5	28.5	48.8	55.0	0.89
TP52	20	4.5	28.5	24.2	41.4	52.0	0.80
TC24	20	6	32.0	26.0	33.4	55.0	0.61
TC42	30	3	25.0	25.0	64.2	52.5	1.22
TP43	35	2@4	22.7	22.7	87.4	78.4	1.11
From Ref. 1: f'_c = 4 ksi, b_f = 20 in., d_f = 5 in., B = 6 in., $A_v f_y$ = 13.2k							
B2-T4	30	6	27.6	27.6	30.4	49.0	0.62
B3-T2	20	4	23.8	21.9	36.1	42.5	0.85
B3-T3	20	6	27.6	23.8	26.2	43.5	0.60
B3-T4	12	6	27.6	19.8	21.8	32.3	0.67
						Average	0.87
						Mean	0.85

quantity $A_v f_y/s$ for a given amount of concentrated load P_u applied to the flange

$$\frac{A_v f_y}{s} \geq \frac{2P_u - 8\sqrt{f'_c}\, b_f d_f}{\phi(B + 2d_f)} \qquad (4.3a)$$

or

$$\frac{A_v f_y}{s} \geq \frac{2P_u}{\phi S} \qquad (4.3b)$$

The larger quantity $A_v f_y/s$ should be used.

Analysis of Flange Punching Shear Strength. The mechanism for a punching shear failure in a flange can form when the applied load exceeds the tensile strength of the concrete along the surface of the truncated pyramid indicated in Fig. 19. The value for tensile strength associated with punching shear in concrete has been taken as $4\sqrt{f'_c}$. That stress can be considered as a tensile stress perpendicular to the surface of the truncated pyramid or as a value for shear stress on a prism with sides located at a distance $1/2d_f$ from the edges of a bearing plate in order to derive an expression for the ultimate concentrated force P_u. Call the "inside" perimeter of base plate B_p. The value of B_p is simply the base plate perimeter minus the length of the side at the edge of the T-beam flange.

$$P_p = 4\sqrt{f'_c}\,(B_p + 2d_f)d_f \qquad (4.4)$$

Stirrups that intersect a face of the truncated pyramid can help support the concentrated load if anchorage of the stirrup can be developed above and below the face of the pyramid. With no help from stirrups the magnitude of P_p from Eq. (4.4) is 38.0 kips for specimen TC1, 48.8 kips for TC2 and TC7, and 51.9 kips for the prestressed specimens TP3, TP4, TP5, and TP6. A glance at Table 4.1 reveals that many of the applied forces are only slightly larger than P_p, with isolated instances of ultimate loads far in excess of P_p (Note TC23, TP43, TP54, and TP63). Only in the cases of torsion tests to failure were ultimate loads less than P_p.

The selection of a flange thickness for inverted T-beams should be made adequate to avoid punching failure when the helpful effect of stirrups is neglected as expressed in Eq. (4.4). If the capacity reduction factor ϕ is multiplied by the righthand side of that equation, an expression for minimum flange depth d_f can be derived.

$$d_f \geq \frac{B_p}{4}\left[\sqrt{\frac{2P_p}{B_p^2\,\phi\sqrt{f'_c} + 1}} - 1\right] \qquad (4.5)$$

This cumbersome appearing equation can be applied most readily as a graph with bearing plate interior perimeter B_p versus ultimate load P_p for various values of flange depth d_f. For example, if f'_c is taken as 4000 psi, a chart for minimum depth can be constructed similar to that of Fig. 22.

Analysis of Bracket Failure. Only two test regions appeared to fail as a result of the type of shear friction loss that is referred to as bracket failure in this report. In each case (TP53 and TP43) the test region contained relatively heavy stirrup (hanger) reinforcement with pairs of #3 bars at not more than 4.5 in. centers. Failures appeared to involve a slipping or shearing along the face of the web.

The flexural steel normal to the shearing face must be adequate to develop a normal force large enough to maintain the frictional shear. A shear friction formula endorsed by the ACI Building Code[3] and supported by data from Ref. 1 suggests that the tensile reinforcement A_{vf} normal to the shearing face can be taken simply as the amount required to develop a normal force about 70 percent as large as the applied shear.

Thus
$$A_{vf} \geq \frac{V_u}{1.4f_y} \qquad (4.6)$$

The values of V_u that were reached in the tests reported here ranged as high as 95.0 kips. With values of f_y at 70 ksi, an area of steel A_{vf} had to be 0.97 sq. in. Generally, the transverse reinforcement

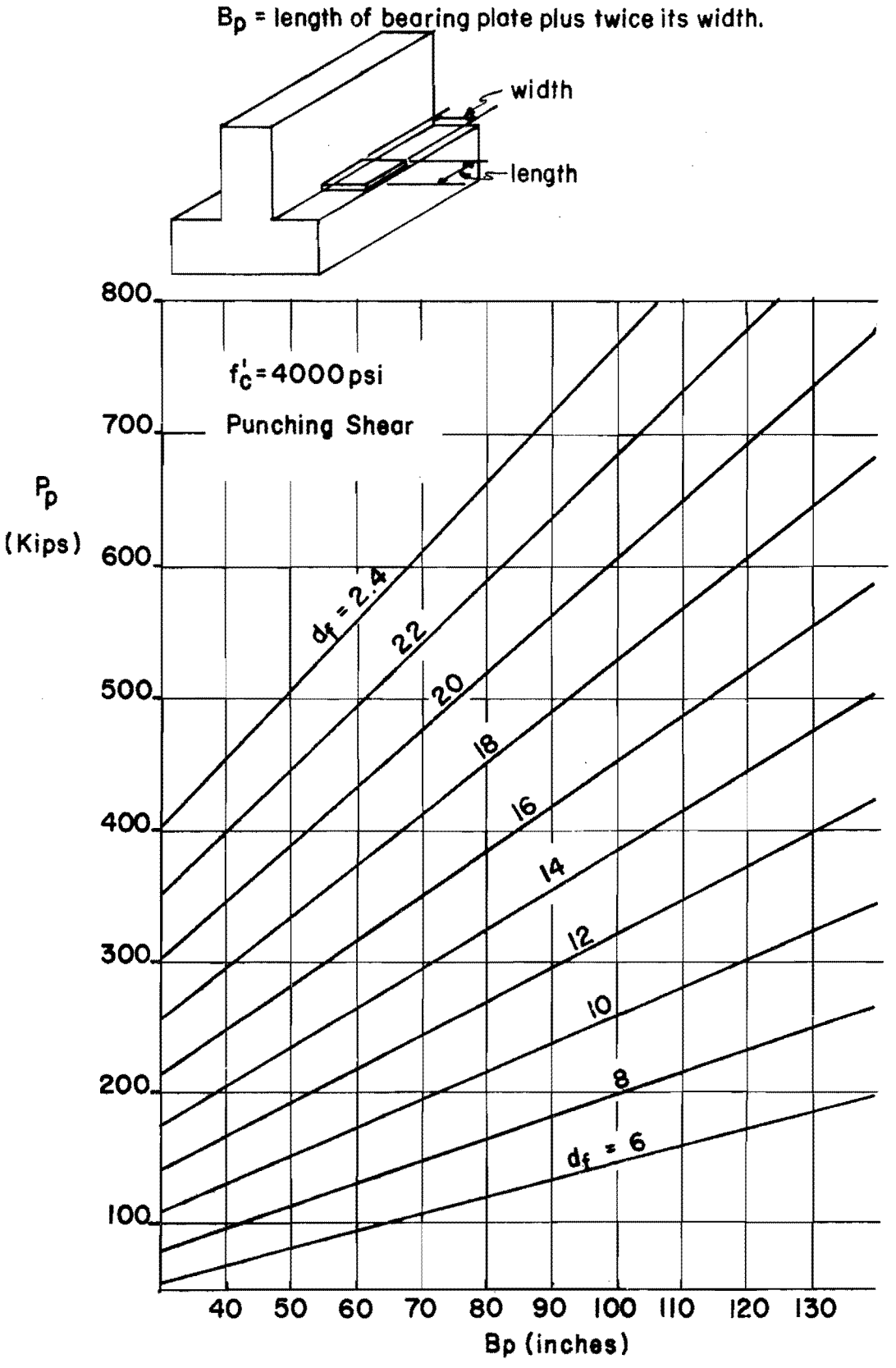

Fig. 22. Punching shear capacity.

at the top of the flange consisted of #3 bars at 3 in. centers. In order for nine #3 bars (A_{vf} = 0.99 sq. in.) to contribute to A_{vf}, there need be only a 24 in. long portion of the flange participating to support the 95 kip load against bracket failure.

It seems apparent that the #3 transverse bars provided more than adequate reinforcement to prohibit shear friction or a bracket-type of failure. For the two tests that appeared to involve a shear friction type of displacement, other weaknesses may have prohibited the full development of available shear friction resistance. Hanger and punching weakness accompanied the bracket-type failure of TP43 and overall torsion, shear, and flexural weakness was reported along with the bracket-type failure of TP53. The punching shear strength involved a mechanism more critical than the shear friction mechanism.

Recommendations of Ref. 1 indicated that transverse bars participate a distance from the edge of the bearing plate two times the dimension "a" from the face of the web to the centroid of the bearing. For specimens in this series of tests, the value of "a" was 4 in. Consequently, all bars within 8 in. from the edge of 6 in. bearing plates could be considered as a part of A_{vf}. Except for load points at the end of specimens, all tests involved eight or more bars within the 22 in. effective width of flange for transverse reinforcement.

Web Failure--Flexural Shear Mode. Flexural shear appeared to be a part of the failure mode that was observed in five tests. It was apparent both from the pattern of applied forces and the response of each of the six test specimens that the flexural shear weakness was a part of the interaction with torsional forces (Table 4.1). Consequently, web failure and flexural shear strength will be discussed only as a component of strength interacting with torsional strength.

Flexural Failure Modes. Flexural failure was observed to be a part of the failure mode in five of the tests. In each of the five cases flexural "failure" in the form of large tension cracks or compression surface spalling was accompanied by evidence of a torsional mode of

failure. Results from the five tests are listed in Table 4.3 together with estimates of cracking moment and the moment at which reinforced concrete specimens should yield.

The maximum moment that was applied to reinforced concrete specimens TC12 and TC72 was considerably below the estimated flexural capacity of each. The estimated yield moment was not reached for either test. Obviously the longitudinal effect of torsional loading was significant for both tests, because some of the longitudinal bars yielded and large cracks could be observed under maximum loads. Flexural cracks first formed without torsional loads when moments were about one-tenth of the ultimate flexural loading.

The maximum moments that were applied to the three prestressed concrete specimens that appeared to be near a limit in flexure (TP31, TP53, and TP62) were within 10 percent of the ultimate flexural strength under flexure alone. Changes in flexural behavior due to torsion were must less apparent in prestressed than in ordinary reinforced concrete specimens. The initial cracking moment for prestressed members was almost 40 percent of the ultimate moment, whereas the cracking moment for reinforced concrete members was only 7 percent of the ultimate moment. After cracking begins, the internal mechanisms that resist flexure continually change for each new condition of load. The superposition of torsional forces should be expected to alter the distribution of longitudinal forces moreso in extensively cracked, reinforced elements than in prestressed elements with limited cracking.

TABLE 4.3. FLEXURAL FAILURE TEST DATA

Test No.	P_u	Computed Moments			Observed Moments	
		Cracking	Yielding	Ultimate	Maximum	Yield
	k	in.-k	in.-k	in.-k	in.-k	in.-k
TC12	39	- 300	-4150	-4600	-2940	None
TC72	52.5	- 300	-4150	-4600	-3750	-3570
TP31	52	+1600	No	+4480	+4160	+3200
TP53	57	+1600	Estimate	+4500	+4020	+3710
TP62	50	-1800	--	-4130	-4200	-2520

There were no flexural failures. Flexural strength for these tests cannot be considered independent from torsion. The indices of flexural behavior are taken from strain gages on longitudinal bars, particularly those bars located in the corners of the specimen. The warping of cross sections due to torsion has a significant effect on corner strains in the longitudinal direction. The significance of the effect becomes more obvious after concrete cracks from excess longitudinal tension. The appearance of flexural distress can and did occur, but longitudinal stress from torsion was a major part of such an appearance.

Torsional Failure Mode. Torsion loads without flexural shear or the accompanying flexural moment were applied to ten test regions, seven of which failed in a mode which appeared to be exclusively a torsional failure. The seven torsion failure modes were obtained in test regions adjacent to a "clamped" support with loads applied to the top and bottom of the flange at a cantilevered portion near the end of each specimen. Test results are listed in Table 4.4, together with a comparison of analytical and measured torsion loads. There is a remarkable similarity among the torsion failure loads, with the maximum value of 1090 in.-k only 16 percent higher than the lowest measured value of 910 in.-k at failure.

TABLE 4.4. PURE TORSION STRENGTH ANALYSIS

Test No.	Measured T_u in.k	Web #3 Spa. in.	Flange #2 Spa. in.	Est.T_t Eq.(4.7) in.-k	T_o ACI in.-k	Limit T_oACI in.-k	$\frac{T_u}{T_{oACI}}$	$\frac{T_u}{\text{Limit}T_o}$	1.5 Limit T_o
TC13	910	4	3	1020	545	582	1.67	1.56	873
TC73	1034	4	2@3	1190	710	654	1.46	1.58	981
TP32	1090	2@4.5	3	1760	852	717	1.28	1.52	1075
TP33	1090	2@4.5	3	1760	852	717	1.28	1.52	1075
TP55	960	2@9	3	950	560	720	1.71	1.33	1080
TP64	1090	4	2@3	1190	721	696	1.51	1.57	1044
TP65	1060	3	2@3	1490	831	696	1.28	1.52	1044

The similarity among failure loads suggests that for inverted T-beams there may be a limit to torsion strength that is independent of the amount of transverse reinforcement and independent also of the amount and form of longitudinal reinforcement. A recommended[2,3] upper limit to torsion strength should be taken as the torsion that generates a nominal stress of $12\sqrt{f'_c}$. The recommended upper limit is given as ACI Limit in Table 4.4. The upper limit based on a torsion stress of $12\sqrt{f'_c}$ was approximately 60 percent of the observed ultimate torsion actually applied. Estimates of flexural capacity for each specimen are shown in Table 4.5, and it should be noted that flexural capacities were all between 4130 and 4600 in.-k.

An estimate of the torsion capacity can be derived from an adaptation of Lessig's truss analysis.[6] Two possible failure modes were illustrated in Fig. 17. A view of the cross section from a longitudinal axis would indicate that torsional capacity can be no greater than that dependent upon the yield forces on stirrup-type reinforcement. Let $A_w f_y$ be the strength of web reinforcement located at a spacing s_1, and let $A_f f_y$ be the strength of U-shaped flange reinforcement, all of which was located at a spacing s_2 = 3 in. centers. The number of stirrups that are intercepted by a torsion crack is related to the angle between a verfical plane and the diagonal cracks. Assuming 45-degree cracks, the torsional capacity T_t based only on transverse reinforcement becomes

$$T_t = A_w f_y \frac{d_1}{s_1}(x_1 + y_1) + A_f f_y \frac{d_2}{s_2}(y_2 + 2x_2) \qquad (4.7)$$

in which x_1 is the horizontal distance between stirrup legs, y_1 is the vertical distance between stirrup legs, y_2 is the horizontal distance, and x_2 the vertical distance between U-shaped flange stirrup legs. Values of ultimate torsion determined with Eq. (4.7) are shown in Table 4.4. Also shown are values of ultimate pure torque determined on the basis of Eqs. (11-16), (11-17), and (11-19) of the ACI Building Code.[3] Finally, Table 4.4 also contains values of the ACI upper limit to torsion strength taken simply as a stress $12\sqrt{f'_c}$ times the torsion shape factor.

The measured values of ultimate torque in tests TP32, TP33, and TP65 were appreciably less than those estimated with Eq. (4.7) based on the assumption that side face cracks occurred at an angle of 45 degrees from the vertical axis. Obviously, for the specimens that failed at smaller values of torque, the angle had to be less than 45 degrees and fewer stirrups were able to help resist the torsion force. Apparently, stirrups that were spaced closer than 4 in. became ineffective in resisting torsion. When stirrup spacing was 4 in., the ratio $A_t f_y / b_w s$ was equal to 0.24 ksi. Possibly the effectiveness of a greater amount of stirrup reinforcement could have been improved through an increase in flexural capacity, but there was no evidence from these tests to encourage that possibility.

The torsion capacities that were determined on the basis of equations of the ACI Building Code[3] gave values less than those observed for all seven tests. The T_o values were computed to include the torsional strength of #3 bars in the web and #2 bars in the flange, plus the torsional strength of the concrete. If the lower of the ultimate torque estimates based on ACI equations were used as a limit, the ratios between measured torque and the ACI limit torque would remain within values 1.52 to 1.71. Thus, for these seven tests of inverted T-beams, the ACI torsion limits seem to be only two-thirds as high as experimental values. The limiting torque equations based on ACI regulations can be expressed as the lower of the values T_o computed for inverted T-beams with web dimensions b_w and h_w and flange dimensions b_f and h_f:

$$T_o = (4\sqrt{f'_c})[b_w^2 h_w + b_f h_f^2] \qquad (4.8)$$

$$T_o = 0.8\sqrt{f'_c}\,[b_w^2 h_w + b_f h_f^2] + \frac{A_t}{3s} f_y y_1 (2x_1 + y_1) \qquad (4.9)$$

A limit to the effectiveness of web stirrups would be reached when the stirrup capacity reaches 80 percent of the T_o value of Eq. (4.8). A maximum amount of effective stirrup reinforcement for torsion can be derived

$$\frac{A_t f_y}{b_w s} \leq \frac{9.6\sqrt{f'_c}}{y_1(2x_1 + y_1)} \left[b_w h_w + \frac{b_f}{b_w} h_f^2\right] \qquad (4.10)$$

The ratio from Eq. (4.10) was 0.35 ksi for specimens used in these tests.

Combined Flexure and Torsion. Altogether 17 of the tests performed involved torsion plus flexural moment. Nine tests involved positive moment (tension in the bottom flange) and eight tests included negative moment plus the torsion loading. Eight tests were performed on prestressed concrete and nine involved no prestressing. The strength results are listed in Table 4.5 in the columns marked Observed.

Computed strength estimates also are shown in Table 4.5. In the absence of any torsion stress, a flexural shear capacity V_o may be taken as the shear strength of concrete plus the strength of stirrups according to the equation derived from the ACI Building Code.[3]

$$V_o = 3.5\sqrt{f'_c}\, b_w d + A_v f_y \frac{d_w}{s} \qquad (4.11)$$

There is an upper limit of $8\sqrt{f'_c}\, b_w d$ on the amount of shear that can be assigned to stirrups in the second component of the sums in Eq. (4.11). In effect the limit on stirrup shear capacity can be used to set an upper limit on V_o as

$$V_o \leq 11.5\sqrt{f'_c}\, b_w d \qquad (4.12)$$

Both the V_o quantity from Eq. (4.11) and the upper limit value are given in Table 4.5.

Moment capacity in the absence of torsional force can be evaluated both for prestressed and for nonprestressed cross sections according to well-established procedures.[2,7,8,9] Moment capacities for measured yield strengths of deformed bars and the nominal strength of prestressing strands are shown as values M_o in Table 4.5.

Torsion strength in the absence of flexural shear was discussed in the description of failure modes. Estimates of torsion capacity in

TABLE 4.5. ANALYSIS OF COMBINED TORSION AND FLEXURE

Specimen Test	Observed			Computed Strength					Ratios		
	V_u	M_u	T_u	V_o Eq. (4.11)	V_o Limit Eq (4.12)	M_o	T_o Eq. (4.8)	T_o Eq. (4.9)	V_u/V_o	M_u/M_o	T_u/T_o
	k	in.-k	in.-k	k	k	in.-k	in.-k	in.-k			
TC11	98	2340	232	89	~~119~~	5300	368	~~582~~	1.10	0.44	0.63
TC21	125	4375	340	89	~~118~~	5300	383	~~653~~	1.40	0.83	0.89
TC22	115	4025	300	89	~~118~~	5300	383	~~653~~	1.29	0.76	0.78
TC23	135	4725	380	~~141~~	118	5300	635	~~653~~	1.14	0.89	0.60
TC71	125	3750	340	89	~~118~~	5300	383	~~654~~	1.40	0.71	0.89
TP31	124	4340	336	~~165~~	129	4500	~~852~~	717	0.96	0.96	0.47
TP51	130	4550	360	110	~~130~~	4500	456	~~720~~	1.18	1.01	0.79
TP52	124	3720	336	110	~~130~~	4500	456	~~720~~	1.18	0.83	0.74
TP53	134	4020	376	~~179~~	130	4500	456	~~720~~	1.03	0.89	0.82
TC12	98	2340	464	89	~~119~~	4600	368	~~582~~	1.10	0.51	1.26
TC24	130	2600	720	89	~~118~~	4600	383	~~653~~	1.46	0.56	1.88
TC25	130	2600	720	89	~~118~~	4600	383	~~653~~	1.46	0.56	1.88
TC72	125	3750	680	114	~~118~~	4600	509	~~652~~	1.10	0.81	1.33
TP41	120	4200	640	~~194~~	125	4130	~~894~~	692	0.96	1.02	0.98
TP42	125	4375	680	~~143~~	125	4130	642	~~692~~	1.00	1.06	1.06
TP61	130	4550	720	~~194~~	126	4130	~~894~~	696	1.03	1.10	1.03
TP62	120	4200	640	116	~~126~~	4130	517	~~696~~	1.03	1.02	1.24

accordance with provisions of the ACI Building Code were found to be the most consistent, albeit approximately 60 percent less than the observed capacities. Torsion strength T_o was computed for each test region according to Eq. (4.9) and the upper limit capacity given by Eq. (4.8), and the results are tabulated in Table 4.5.

Using as the computed strength in shear the lower of the computed values V_o and also using the lower of the two computed values of T_o, ratios between observed strength and computed strength were determined. The ratios are shown in Table 4.5 in the righthand columns, and the ratios are plotted with some interaction graphs in Fig. 23.

Results from only two tests--TP31 and TP41--fell within the square that is indicated by cross-hatched lines. Those two test results were within 4 percent of one of the cross-hatched lines. Basically then, the data from this test series suggest that if strength limits of Refs. 2 and 3 (ACI and AASHO) are used, any weakness due to combined shear and torsion interaction could be ignored for strength. Cross sections that are proportioned for adequate shear acting alone, adequate for torsion acting alone, and adequate for moment acting alone would not be likely to fail if both the design shear and design torsion acted simultaneously.

Evidence from these tests clearly indicated that there was an upper limit to the amount of stirrup reinforcement that effectively contributed to strength in torsion. The upper limit could be expressed in terms of the dimensions of the cross section and the compressive strength of concrete as:

$$\max T_o = 18 \sqrt{f'_c} \Sigma x^2 y \qquad (4.13)$$

The same upper limit applies equally well for both prestressed and non-prestressed specimens.

In view of the "accepted" notion that there must be some strength relationship between shear and torsion, a more appropriate conclusion should acknowledge first the undervalued torsion strength estimates of T_o. The circular arc of Fig. 23 represents the interaction function

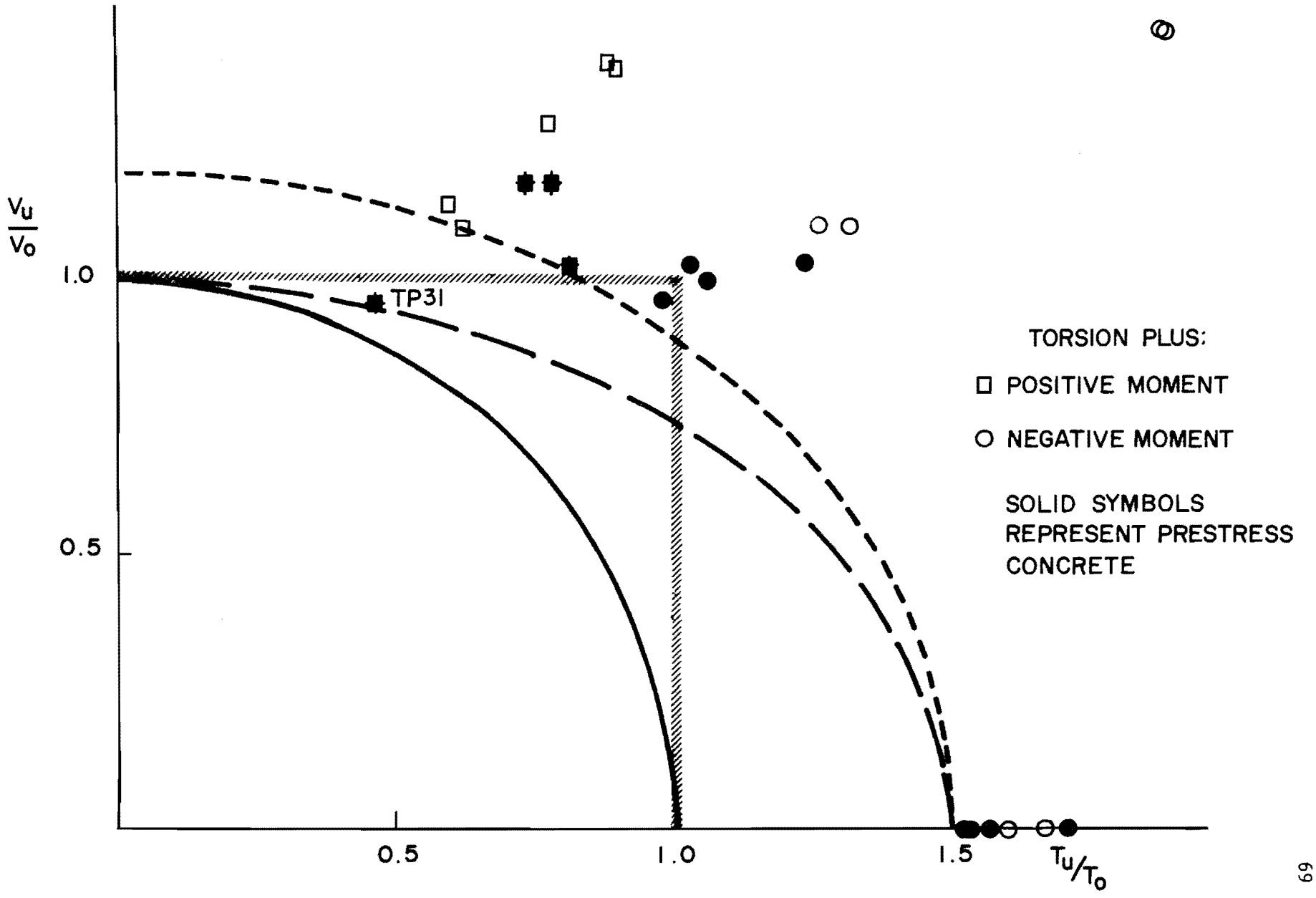

Fig. 23. Combined shear and torsion.

$$\left(\frac{V_u}{V_o}\right)^2 + \left(\frac{T_u}{T_o}\right)^2 = 1 \qquad (4.14)$$

The dashed line arc represents the interaction function

$$\left(\frac{V_u}{V_o}\right)^2 + \left(\frac{T_u}{1.5T_o}\right)^2 = 1 \qquad (4.15)$$

and the dotted line represents an interaction function

$$\left(\frac{V_u}{1.2V_o}\right)^2 + \left(\frac{T_u}{1.5T_o}\right)^2 = 1 \qquad (4.16)$$

All data points, including those for pure torsion tests, fall outside of the curve for Eq. (4.15) which employs a 50 percent increase in the predicted torsion capacity based on the ACI recommendations. Only one test involved a failure inside the strength interaction function expressed by Eq. (4.16) for which flexural shear estimates were increased 20 percent and torsional shear estimates were increased 50 percent. The results of these tests clearly indicate that the torsion strength estimates derived from ACI Building Code recommendations could be increased 50 percent.

The torsion capacity estimates of the ACI Building Code assign part of the pure torque strength to concrete and the remainder to transverse reinforcement as expressed in Eq. (4.9). The truss analysis formulated in Eq. (4.7) neglects torsion strength in concrete, assigning all resistance to yielded transverse bars that penetrate 45-degree side cracks. A comparison of the equations indicates that the ACI strength formulation for transverse reinforcement in the web only gives values lower than the truss analysis of Eq. (4.7) by the ratio $(x_1 + 2y_1)/3s$, if y_1 were taken equal to d. Estimates based on Eq. (4.7) were higher than the upper limit of Eq. (4.13) for all pure torsion tests, and the reliability of Eq. (4.7) cannot be deduced from these tests. However, the relationships do encourage a search for a formula that attributes to transverse reinforcement more strength than that permitted by the ACI Building Code Eq. (11-9).

On the basis of data from these tests and observations of beams as each was loaded to failure, the interaction of flexural shear and torsional shear appeared to be influenced significantly by concrete strength and concrete stiffness only prior to the development of diagonal cracking. After cracks developed, the concrete served primarily to equilibrate in compression the tensile forces on both transverse and longitudinal reinforcement. As cracking extended and rotations increased, the diagonal cracking tended more toward vertical planes. The "pure" shear strength of concrete between reinforcing bars appeared to establish an upper limit to torsional capacity regardless of excess reinforcement. Although it seemed that strength could be evaluated completely in terms of capacity for the reinforcement that penetrated the failure surface, the orientation of the failure surface had to be a function of both the concrete strength and the amount of reinforcement. Consequently, the ACI formulation for interaction between flexural and torsional shear may reflect trends of behavior, but it does not represent an accurate mechanism for evaluating capacity.

CHAPTER 5

RECOMMENDED PRACTICE FOR DESIGN

The six modes of failure that were discussed in the preceding chapter constitute all of the strength factors that need to be considered for the design of inverted T-beam bent cap girders. The overall strength of the inverted T-beam must be adequate to support ultimate flexure, flexural shear, and torsional shear forces and any possible combination of such forces. The local strength of inverted T-beam components must be adequate to support forces that are applied as concentrated loads on the flange. Locally, the flange must be deep enough to avoid punching shear weakness, the transverse flange reinforcement must be strong enough to maintain shear friction resistance at the face of the web, and web stirrups must be sufficient to act as hangers which transmit flange loads into the web.

Service load conditions of deflection and crack control may be more significant than strength requirements for some components of design. Decisions regarding the overall depth of web and the distribution of tensile reinforcement both for flexure and for stirrups acting as hangers may involve service load conditions of behavior. The height of web above the top of the flange is determined by the required depth of the stringer to be supported on the flange. A minimum depth of the flange itself can be derived from punching shear requirements, but additional depth may be appropriate to provide enough flexural stiffness for the overall member. The thickness of the web b_w can be selected for adequate strength in shear and torsion, or it may be determined by placement requirements of flexural reinforcement. It is beyond the scope of research reported here to define all parameters appropriate for design decisions. Various minima can be suggested from performance requirements observed in this project and the preceding study of inverted T-beams.

Flange Thickness for Punching Shear

The strength of a flange in punching shear was described in Eq. (4.4) on the assumption that no stirrups or flange bars augment the punching shear strength. Introduction of the capacity reduction factor ϕ and a rearrangement of Eq. (4.4) yields the following expression for minimum flange depth $_{min}d_f$ below a bearing pad of inside perimeter B_p and supporting an ultimate load P_u.

$$_{min}d_f = \frac{B_p}{4}\left(\sqrt{\frac{2P_u}{1 + B_p^2\,\phi\sqrt{f'_c}}} - 1\right) \qquad (4.5)$$

A design aid graph for Eq. (4.5) is provided in Fig. 22. The punching shear failure mechanism was found to be more critical than the shear friction mechanism described for inverted T-beams in Ref. 1.

Transverse Reinforcement in the Flange

Reinforcement must be placed across the top half of the flange to resist flexural tension at the face of the web and to ensure enough pressure perpendicular to the face of the web to sustain shear friction stresses. The amount of such steel A_{vf} should satisfy the following relationship when a capacity reduction factor ϕ = 0.85 is used.

$$A_{vf} \geq \frac{P_u}{1.2f_y} \qquad (5.1)$$

Only two-thirds of A_{vf} should be placed in the top layer of flange reinforcement. The remaining one-third of A_{vf} should be placed in one or more layers in the top half of the flange thickness. If the distance from the face of the web to the center of a bearing plate is designated as "a", all of the reinforcement within a distance 2a from the edge of a bearing plate can be considered as a part of A_{vf}.[1]

The shear friction requirements for A_{vf} will require more transverse reinforcement than will flexural considerations if the distance "a" is less than half the flange depth d_f. For values "a" greater than $0.5d_f$,

the top layer of transverse reinforcement should provide within a distance 2.5a each side of the bearing plate an area A_s'.

$$A_s' \geq \frac{1.4P_u a}{f_y d_f} \tag{5.2}$$

In addition, an area of steel at least $0.5A_s'$ should be placed in one or more layers below A_s', but in the top half of the flange thickness.

In order to ensure the development of yield stresses in transverse bars, it is necessary in most circumstances to weld the ends of transverse bars to an anchor bar at the exterior face of the flange and perpendicular to the transverse bar.

Design of Stirrups

Vertical reinforcement in the web must be adequate to transmit flange loads into the web, and the same reinforcement must serve also to sustain flexural and torsional shear on the inverted T-beam. Stirrups act as hangers to transmit flange loads into the web, and there appears to be no significant interaction among hanger loads and flexural or torsional shear forces in the stirrups.

Hangers

For all of the specimens observed in this research, the flange was stiff enough to redistribute hanger forces among as many hangers as the shear capacity of the flange could support. However, the hangers that were nearest to the concentrated forces that were applied to the flange occasionally reached yield stresses under service load conditions. In order to limit the size of cracks that form when hangers reach high stress levels, it seems desirable to limit to $0.5f_y$ the nominal service load stress of hangers within the distance "a" from edges of the base plate.

There are, therefore, three conditions for which stirrups must be adequate. The three conditions are expressed in the three equations for the area A_v for two legs of a stirrup at a spacing of s in.

$$\frac{A_v}{s} \geq \frac{2P_u - 8\sqrt{f'_c}\, b_f d_f}{\phi\, f_y (B + 2d_f)} \tag{5.3a}$$

$$\frac{A_v}{s} \geq \frac{2P_u}{\phi f_y S} \tag{5.3b}$$

$$\frac{A_v}{s} \geq \frac{3(P_D + P_L)}{f_y (B + 3a)} \tag{5.4}$$

The first two equations show strength requirements and the third is a serviceability condition. The largest value A_v/s must be used for design of hangers.

Web Shear and Torsion

Stirrups also serve as vertical reinforcement of a T-beam web that is subjected to combined flexural and torsional shear. There was no evidence that local hanger forces should be superimposed on the web shear forces. The present recommendations of the ACI Building Code[3] and AASHO[2] regulations definitely appeared to be safe and appropriate for the assessment of flexural shear behavior. However, the torsion strength recommendations of the ACI Building Code appeared to lead to strength estimates considerably below those observed in these tests.

Since the ACI Building Code procedures gave strength estimates no greater than 67 percent of those observed, and since the participation of plain concrete constituted less than 25 percent of the analytical total torsional strength of members, it seems needlessly complex to encourage the use of an interaction formula to reduce the permissible ultimate torsional strength of plain concrete as flexural shear forces increase. Instead, there was evidence that if an interaction between flexural shear capacity and torsional shear capacity were to be assumed, it could employ

for concrete some values of ultimate flexural shear stress v_c and ultimate torsional shear stress v_{tc} which are taken as constant values that are independent of the ultimate total stress v_u for flexural and v_{tu} for torsional shears.

Even though it has been observed that the ACI formulation for torsional strength in transverse reinforcement undervalues such reinforcement, the relationship expressed by Eq. (4.9) must be recommended for design until documentation for a better equation is available.

$$\frac{T_o}{\phi} = 0.8\sqrt{f'_c}\,[b_w^2 h_w + b_f h_f^2] + \frac{A_t}{3s} f_y y_1 (2x_1 + y_1) \qquad (5.5)$$

The most likely design circumstance for bridge bent girders involves a flexural shear design force that is largest when torsion is small because traffic will load stringers both sides of the girder web. When torsion is a maximum, traffic will load stringers on only one side of the web, and flexural shear must be less than the maximum value. Consequently, a logical design procedure might begin with the proportioning of stirrups solely on the basis of maximum flexural shear requirements V_o (wherever those necessitate more stirrups than do hanger requirements). Next, Eq. (5.5) should be employed to evaluate T_o. Finally, the reduced value of shear V_u accompanying the design torque T_u can be substituted into the interaction Eq. (4.14), here repeated as a necessary inequality for design.

$$\left(\frac{V_u}{V_o}\right)^2 + \left(\frac{T_u}{T_o}\right)^2 \leq 1 \qquad (5.6)$$

If the inequality is not satisfied, then more stirrups would be needed. An estimate of the required amount of extra transverse steel could be taken as the ratio by which the left side of Eq. (5.6) exceeds unity. It remains important and necessary to check that upper limit flexural and torsional shear capacities expressed by Eq. (4.12) and Eq. (4.8) are not exceeded by V_o and T_o forces used in Eq. (5.6).

Evidence from all tests reported here indicated that the same design procedure and equations for stirrups in nonprestressed concrete

apply equally well for prestressed concrete members. The role of longitudinal reinforcement could not be identified specifically from tests conducted in this research. There was an indication that the role of longitudinal steel was much more significant in nonprestressed members than in prestressed members subjected to torsion.

It would seem reasonable to require that the strength of longitudinal reinforcement in a cross section subject to pure torque be at least as great as the strength of transverse reinforcement that would intercept a 45-degree diagonal crack through the member. For prestressed concrete l o g i c would require that the level of prestress be such that there is enough flexural "reserve" in both tension and in compression to equal the strength of transverse reinforcement that would intercept the 45-degree diagonal crack. Flexural "reserve" is the total amount of compression force or tension force that can be superimposed on prestressing a n d flexural forces before spalling in compression or cracking in tension can occur.

Inverted T-beams are not likely to be subjected to pure torque. The need for supplemental longitudinal reinforcement to help flexural reinforcement to resist torsion will be apparent only for those cases in which the inequality of Eq. (5.6) is not satisfied. If the area of transverse reinforcement must be increased in order to satisfy Eq. (5.6), some supplemental longitudinal steel A_ℓ with a capacity equal to the strength of "extra" transverse steel A_t' should be provided. If the yield strength of A_ℓ and A_t' is the same,

$$A_\ell = 2A_t' \left(\frac{b_w d}{s}\right) \tag{5.7}$$

The area of longitudinal steel A_ℓ should be distributed among the four corners of the web, and it must be added to flexural reinforcement both for nonprestressed and for prestressed members.

R E F E R E N C E S

1. Furlong, Richard W., Ferguson, Phil M., and Ma, John S. "Shear and Anchorage Study of Reinforcement in Inverted T-Beam Bent Cap Girders," Center for Highway Research Report No. 113-4, The University of Texas at Austin, July 1971.

2. Standard Specifications for Highway Bridges, Adopted by the American Association of State Highway Officials, Eleventh Edition, 1973.

3. Building Code Requirements for Reinforced Concrete (ACI 318-71), American Concrete Institute, Detroit, 1971.

4. Kriz, L. B., and Raths, C. H. "Connections in Precast Structures--Strength of Corbels," Portland Cement Association Journal, Vol. 10, No. 1, February 1965.

5. Furlong, Richard W., Wong, Wing-Cheung, and Mirza, Sher Ali. "An Investigation of Creep due to Bond between Deformed Bars and Concrete," Center for Highway Research Report No. 113-5F, The University of Texas at Austin, August 1971.

6. Lampert, Paul, and Collins, Michael P. "Torsion, Bending, and Confusion--An Attempt to Establish the Facts," Journal of the American Concrete Institute, August 1972.

7. Ferguson, Phil M. Reinforced Concrete Fundamentals, Third Edition, John Wiley & Sons, Inc., New York, 1973.

8. Winter, G., and Nilson, A. H. Design of Concrete Structures, Eighth Edition, McGraw-Hill, New York, 1972.

9. Wang, Chu-Kia, and Salmon, Charles G. Reinforced Concrete Design, Second Edition, Intext Educational Publishers, New York, 1973.